의학박사 학위논문

Hepatoprotective effects of ursodeoxycholic acid explored via global metabolomics and bile acid profilings

글로벌 대사체 분석 및 담즙산 프로파일링을 통한 우루소데옥시콜산의 간기능 보호기전 규명

2020 년 2 월

서울대학교 대학원
의과학과 의과학전공
김 다 정

A thesis of the Degree of Doctor of Philosophy

글로벌 대사체 분석 및 담즙산 프로파일링을 통한 우루소데옥시콜산의 간기능 보호기전 규명

Hepatoprotective effects of ursodeoxycholic acid explored via global metabolomics and bile acid profilings

February 2020

Major in Biomedical Sciences
Department of Biomedical Sciences
Seoul National University Graduate School
Da Jung KIM

글로벌 대사체 분석 및 담즙산 프로파일링을 통한 우루소데옥시콜산의 간기능 보호기전 규명

지도 교수 유 경 상

이 논문을 의학박사 학위논문으로 제출함
2020년 2월

서울대학교 대학원
의과학과 의과학전공
김 다 정

김다정의 의학박사 학위논문을 인준함
2020년 2월

위 원 장 강 인 진 (인)
부위원장 유 경 상 (인)
위 원 김 혜 선 (인)
위 원 조 주 연 (인)
위 원 윤 영 감 (인)

Hepatoprotective effects of ursodeoxycholic acid explored via global metabolomics and bile acid profilings

by
Da Jung KIM

A thesis submitted to the Department of Biomedical Sciences in partial fulfillment of the requirements for the Degree of Doctor of Philosophy in Medicine at Seoul National University College of Medicine

February 2020

Approved by Thesis Committee:

Professor Jinju Jang **Chairman**
Professor Kyung-Sang Yu **Vice chairman**
Professor Hye-Sun Kim
Professor Joo-Youn Cho
Professor YoungRan Yoon

ABSTRACT

Hepatoprotective effects of ursodeoxycholic acid explored via global metabolomics and bile acid profilings

Da Jung KIM

Department of Biomedical Sciences

Seoul National University Graduate School

Introduction: Ursodeoxycholic acid (UDCA), a secondary bile acid, is a metabolic byproduct of intestinal bacteria and has long been used as a hepatoprotective treatment. The molecular mechanism governing its activity remains unclear, but it has been proposed to regulate the bile acid pool and lower bile acid hydrophobicity. The purpose of this study was to investigate the mechanisms underlying the therapeutic effects of UDCA by using metabolomics and metagenomics analyses in healthy subjects and in patients with liver dysfunction.

Methods: A total of 60 subjects, 24 younger adults, 16 elderly and 20 patients with liver dysfunction were enrolled in this study and underwent randomization. Younger adults were administered UDCA at dosage of 400, 800, or 1200 mg daily for 2 weeks. Elderly were administered UDCA at dosage of 400 or 800 mg daily for 2 weeks. For patients with liver dysfunction, UDCA 600 mg or vitamin E 800 IU were treated daily for 8 weeks. Blood and urine samples were collected at pre- and post-dose. Liquid chromatography coupled with quadrupole time-of-flight mass spectrometry and gas chromatography coupled with time-of-flight mass spectrometry were used for global metabolomics

profiling. Quantitation of 15 bile acids were performed using liquid chromatography tandem mass spectrometry. Metagenome profiling was performed by sequencing 16s ribosomal DNA (rDNA) and assessing microbial codiversity. To identify discriminative markers before and after treatment, multivariate and univariate analyses were used.

Results: In healthy younger subjects, alanine transaminase score (ALT), aspartate aminotransferase (AST) and serum miR-122 levels decreased significantly after 2 weeks of UDCA treatment. Hydrophobic bile acid (tauro-deoxycholoic acid) were significantly reduced after the treatment. Through LC- and GC-based metabolomic profilings, forty differential metabolites belonging to amino acid, flavonoid and fatty acid were identified in plasma and urine samples. In healthy elderly subjects, there was a decreased tendency of liver function scores including ALT and AST upon the UDCA administration however, only the ALT score in UDCA 400 mg group was shown to be statistically significant. No significant changes in bile acid profiling and untargeted metabolomics were observed except for up-regulation of UDCA and its conjugates. In the study of liver dysfunction patients, UDCA significantly improved liver function test values, including ALT, AST, gamma-glutamyl transferase scores and serum miR-122 levels after 8 weeks of treatment and was also effective in reducing hepatic hydrophobic bile acid (deoxycholic acid). To better understand its protective mechanism, a global metabolomics study was conducted. As a result, UDCA regulated uremic toxins, antioxidants, and phenylalanine/tyrosine metabolic pathways. The microbiome, including

Lactobacillus and *Bifidobacterium* species, was found to contribute using metagenome analysis of bacteria-derived extracellular vesicles.

Conclusions: : UDCA treatment regulates liver function scores, hydrophobic bile acids including deoxycholic acid, serum miR-122, levels of metabolites belonging to various metabolic pathways, and microbial composition thus, the treatment is effective in improving liver function.

* Part of this work has been published in *Scientific Reports* (Da Jung Kim, et al. Sci. Rep. 8, 11874 (2018). DOI: 10.1038/s41598-018-30349-1) and *Metabolomics* (Da Jung Kim, et al. Metabolomics. (2019) 15:30. DOI: 10.1007/s11306-019-1494-5).

Keywords: Ursodeoxycholic acid, metabolomics, metagenomics, bile acid profiling, hepatoprotective effect

Student number: 2015-31231

CONTENTS

LIST OF TABLES

LIST OF FIGURES

LIST OF ABBREVIATION

ALP	alkaline phosphatase
ALT	alanine transaminase
AST	aspartate transaminase
BA	bile acid
CA	cholic acid
CDCA	chenodeoxycholic acid
DCA	deoxycholic acid
EV	extracellular vesicle
FXR	farnesoid X receptor
GC-TOFMS	gas chromatography system coupled with time-of-flight mass spectrometry
GGT	gamma-glutamyl transferase
GUDCA	glycoursodeoxycholic acid
LC-QTOFMS	liquid chromatography system coupled with quadrupole-time-of-flight mass spectrometry
NAFLD	non-alcoholic fatty liver disease
PBC	primary biliary cirrhosis
PCA	principal component analysis
TDCA	taurodeoxycholic acid
TUDCA	tauroursodeoxycholic acid
UDCA	ursodeoxycholic acid

INTRODUCTION

Ursodeoxycholic acid (UDCA) is a steroid bile acid extensively used to treat cholesterol gallstones and primary biliary cirrhosis (PBC). UDCA is clinically predicted to improve biochemical parameters via its therapeutic effects. But its therapeutic efficacy remains still controversial [1, 2]. A recent study demonstrated that two years of UDCA treatment effectively reduced liver function scores in Indian NAFLD patients [3]. Numerous mechanistic studies have been conducted on UDCA; however, they have not yielded convincing evidence regarding UDCA-mediated hepatoprotection. For instance, the replacement of potentially toxic hydrophobic endogenous bile acids is theoretically considered the most popular therapeutic strategy [4, 5]. Mechanisms underlying the inhibition of hepatocellular apoptosis have also been evaluated at the cellular level [1, 4, 6]. Moreover, UDCA may exert antagonistic effects on farnesoid X receptor (FXR) to regulate cholesterol and bile acid synthesis in morbid obesity [7]. This antagonistic effect of UDCA however, is still controversial since no published studies showing its direct activity on FXR. According to the profiling serum parameters of obese subjects, inhibition of intestinal FXR activation resulted reduction of fibroblast growth factor 19 (FGF19) in the circulation. Then, hepatic CYP7A1 expression is activated via negative feedback flow therefore, bile acid synthesis is mediated with cholesterol metabolism [8]. Whereas some researchers believed that cholic acid (CA) and chenodeoxycholic acid (CDCA) bind more strongly with the FXR than UDCA [7]. Another study examined the expression of FXR signaling

in the liver following oral administration of UDCA reaching almost 50-fold higher in the serum and found no apparent effects on its expression [9]. Given the state of the existing background knowledge, it is necessary to investigate further detailed therapeutic mechanisms of UDCA for its effective usage.

Global metabolomics—the profiling of metabolites in biofluids, cells, and tissues—has become a routine technique for diagnosing disease and monitoring progression. The identification of numerous biomarkers has furthered current understanding of metabolite systems-level effects, thereby providing novel insights into the underlying mechanisms for various physiological conditions and aberrant processes, including diseases [10]. Despite the widespread use of metabolomics in clinical research, limited information is available regarding the application of metabolomics to study the hepatoprotective effects of bile acids.

Bile acid profiling are frequently used to investigate their pathophysiological effects on the progression of such diseases as Alzheimer's disease [11], inflammatory bowel disease [12], and PBC [13]. Nevertheless, improvement of liver enzyme function, including aspartate transaminase (AST), alanine transaminase (ALT), and alkaline phosphatase (ALP), is a desired effect of UDCA in liver diseases [1, 6, 14, 15]. However, studies of changes in endogenous metabolites and their metabolism upon UDCA administration are lacking in humans, thereby making it difficult to determine the therapeutic mechanisms of UDCA.

Disruption of the gut microbiome affects various in vivo metabolic pathways, including fatty acid and bile acid (BA) metabolism [16]. In obese

animals, the proportion of Firmicutes and Bacteroidetes, two predominant phyla of microbiota in both mice and humans, differs from those in lean animals [16, 17]. Further, UDCA altered the levels of suspected gut microbe-generated metabolites, thus providing initial clues that UDCA may either change the composition of the microbiome or alter the metabolic potential of the gut bacteria [16]. While the efficacy of UDCA to treat PBC has long been discussed, there are few studies regarding its effect on NAFLD.

In the present study, therapeutic effect of UDCA was examined in a dose dependent manner and performed metabolomic profiling related to its therapeutic effects in Korean male subjects. To conduct global metabolomics profiling, a liquid chromatography system coupled with quadrupole-time-of-flight mass spectrometry (LC-QTOFMS) and a gas chromatography-TOFMS (GC-TOFMS) system were used. Quantitation of 15 bile acid species was demonstrated by using a liquid chromatography tandem mass spectrometry (LC-MS/MS). Further, metagenome analyses were performed to establish a link between the drug response and the bacteria-derived metabolites discovered using global metabolomics. For better differentiation of metabolites before and after treatment with UDCA, multivariate principal component analysis (PCA) and univariate analysis were used.

Therefore, the aim of this study was to demonstrate how UDCA treatment influences BA regulation, metabolomics profiling, miRNA expression in healthy younger and elderly subjects (PART I and PART II), and remodeling of the intestinal microbiome to exert hepatoprotective effects against liver damage (PART III).

METHODS

Study design and subjects

PART I. In the study with healthy younger adults, the participants were originally enrolled in a clinical trial to investigate the safety, tolerability, and pharmacokinetics of UDCA and tauro-UDCA in healthy male volunteers (clinicaltrials.gov identifier: NCT02622685). The samples analyzed herein were obtained from participants administered with 400, 800, or 1200 mg UDCA per day for 2 weeks (URSA®, Daewoong Pharmaceutical Co., Ltd.) during this the clinical trial. Participants were aged 19-45 years without any clinical significant underlying disease. Each group was randomly assigned 8 enrolled subjects. The study protocol was reviewed and approved by the Institutional Review Board of Seoul National University Hospital, Seoul, Korea (H-1503-134-660).

PART II. The study in the elderly was approved by the institutional review board (IRB) of Seoul National University Bundang Hospital, Republic of Korea (B-1602-336-005) and is registered at ClinicalTrials.gov (www.clinicaltrials.gov; identifier number is NCT 02789644). The study involving elderly volunteers was a randomized study and included elderly men aged 65-85 years without any clinical significant underlying disease. Subjects were administered a single dose of 400 or 800 mg UDCA at the clinical trial center, followed by the administration of 200 mg UDCA twice daily for 2 weeks through self-medication. Each group was randomly assigned 8 enrolled subjects.

Subjects were excluded from the study if they took prior medication or had a medical history and yielded abnormal findings for clinical laboratory tests, especially hepatic enzyme tests assessing aspartate aminotransferase (AST), alanine aminotransferase (ALT), and γ -glutamyl transferase (γ -GT) levels.

PART III. This study includes the results of clinical trial subjected to patients with liver dysfunction. Participants for this study were originally enrolled as part of a study aiming to evaluate pharmacokinetics and biomarkers after UDCA administration to overweight subjects with liver problems. The study protocol was reviewed and approved by the Institutional Review Board of Seoul National University Bundang Hospital, Seongnam, Korea (IRB number B-1602/336-006) and is registered at clinicaltrials.gov (NCT03000218). Male subjects, aged 20-45 years, were recruited, and the specific inclusion criteria were slightly raised ALT levels (40–200 IU/L) and a body mass index of 25–30 kg/m2. Of the 20 subjects enrolled, 10 were randomly assigned to receive UDCA treatment (300 mg, twice daily), and 10 were assigned to receive vitamin E (GRANDPHEROL, Yuhan Co., Ltd.) treatment (400 IU, twice daily). Vitamin E served as a positive control, known to enhance antioxidant defense mechanisms. Both drugs were administered orally for 8 weeks. During this period, one subject withdrew from the UDCA group for a personal reason after 4 weeks and therefore, was excluded from data analysis.

All the clinical studies were conducted in compliance with the principles of the Declaration of Helsinki and the Guideline of Good Clinical

Practice. All study subjects provided written informed consent before participation in the respective studies.

Sample collection

Blood samples were collected in EDTA-coated vials prior to initial UDCA administration and 24 h after the multiple UDCA administration treatment course for metabolomic analysis and to determine the miRNA, AST, ALT, and γ -GT levels. Urine samples were collected over two 24 h periods, the first starting 24 h prior to first administration and the second starting immediately after the final administration of the treatment course. Plasma was separated via centrifugation (4 °C, 3000 rpm, and 10 min) and stored at − 70 °C until analysis. For miRNA analysis, blood samples were collected in serum-separating tubes, centrifuged (25 °C, 2400 rpm, and 10 min), and stored at − 20 °C until analysis. Urine samples were stored at 4 °C after collection. At 24 h after collection, 10 mL sample aliquots was transferred to Falcon tubes for storage at − 70 °C until analysis.

Serum miRNA measurement

Total RNA was extracted for quantitative analyses of serum miRNAs using an miRNeasy Mini kit (Qiagen, Hilden, Germany) according to the manufacturer's recommendations. Serum (100 μl) was used for the RNA extraction. A synthetic miRNA from Caenorhabditis elegans was included in the sample after homogenization in QIAzol lysis reagent (Qiagen) to validate the RNA

extraction efficiency. cDNA was prepared using an miScript Reverse Transcription Kit II (Qiagen). PCR reaction system (20 μl) contained 10 μl of miScript SYBR Green PCR Master Mix (Qiagen), 4 μl of nuclease-free water, 2 μl of 10× miScript primer assay, 2 μl of 10× miScript Universal Primer, and 2 μl of cDNA template. Amplification was performed using a CFX96 Real-Time System (BioRad, Hercules, CA, USA) under the following conditions: initial denaturation at 95 ºC for 15 min followed by 40 cycles of denaturation for 15 s at 94 ºC, annealing for 30 s at 55 ºC, and elongation for 30 s at 70 ºC. A total exosome isolation reagent (Invitrogen, Carlsbad, CA, USA) was used for exosome isolation from the serum according to the manufacturer's instructions.

Global metabolomics-LC-QTOFMS analysis

Each sample (5 μl) was loaded onto an ACQUITY UPLC BEH C18 (1.7 μm, 2. 1 × 100 mm; Waters Corp., Milford, MA, USA) column held at 40 ℃ and eluted with 0.1% formic acid and 20 mM ammonium formate in water (solvent A) and 0.1% formic acid in methanol (solvent B) with a constant flow rate of 0.4 ml/min and the following gradient conditions: 0−0.1 min, 2% B; 0.1−13 min, 2−98% B; 13−15 min, 98% B; 15−15.1 min, 98−2% B; 15.1−17 min, 2% B. Subsequently, the eluent was introduced into an Agilent 6530 QTOF-MS (Agilent Technologies, Santa Clara, CA, USA). The overall quality of the analysis procedure was monitored using repeat extracts of a pooled plasma or urine sample. Urine samples were analyzed in the negative ESI mode, and plasma samples in the positive ESI mode. The intensity of each ion was

normalized, scaled, z-transformed, and aligned according to retention time through the Mass Hunter Profinder B.08.00 and Mass Profiler Professional (MPP) software package B.14.9 (Agilent Technologies) to generate a normalized data matrix consisting of retention time, m/z value, and normalized peak area.

Global metabolomics-GC-TOFMS analysis

Frozen samples were thawed at 4 °C and 50 µL of each sample was diluted with 1 ml of an acetonitrile:isopropanol:water (3:3:2) mixture. Mixed samples were vortexed for 5 min and centrifuged at 18,341 × g for 5 min at 4 °C. Thereafter, 400 µL of supernatant was evaporated to complete dryness at room temperature and reconstituted to 400 µL with 50% acetonitrile. Centrifugation was then repeated for 5 min at 18,341 × g at 4 °C. The supernatant was then evaporated and the residue was reconstituted with 10 µL of methoxyamine dissolved in pyridine and maintained at 30 °C for 90 min under shaking. After cooling the samples to room temperature, 90 µL of a mixture of MSTFA (N-Methyl-N-(trimethylsilyl) trifluoroacetamide) and FAME (fatty acid methyl esters) was added to each experimental sample and the pooled QC samples. The samples were incubated at 70 °C for 45 min under shaking, then transferred to autosampler vials with glass inserts. Aliquots (1 µL) were then injected in splitless mode into an Agilent 7890A gas chromatograph coupled with a Pegasus HT time-of-flight mass spectrometer (Leco Corporation, St. Joseph, MI). Separation was achieved on a DB-5ms capillary column (30 m × 250 µm i.d., 0.25 µm film thickness; (5%-phenyl)-methylpolysiloxane bonded and

cross-linked; Agilent J&W Scientific, Folsom, CA, USA), with helium as the carrier gas at a constant flow rate of 1.5 mL/min. Oven temperature was initially set to 50 °C for 0.5 min and ramped to 330 °C at a constant rate of 20 °C/min up to 20 min. The intensity of each ion was normalized to the total sum of all detected metabolites using ChromaTof software and then aligned according to retention time (v4.61 Leco Corporation, St. Joseph, MI). Candidates extracted from multivariate analysis (refer to statistical analysis section) were selected for using similarity, reserve, and probability values (above 700, 800, and 3000, respectively). Thereafter, the data set was matched with existing metabolite in libraries.

Quantitation of bile acids

Plasma samples were prepared according to the manufacturer's instructions. For liquid chromatography-tandem mass spectrometry (LC-MS/MS) analyses, 10 μL of diluted filtrate was injected into an Agilent 1200 series high-performance liquid chromatography (HPLC) system (Agilent Technologies, Santa Clara, CA) consisting of a binary pump (G1312A) and an autosampler (G1367B) with a thermostat (G1330B) set at 10 °C. Separation was achieved on an analytical column using the Biocrates® Bile Acids Kit (Biocrates Life Science AG, Innsbruck, Austria) equipped with an AJ0-4287 SecurityGuard™ ULTRA cartridge for C18 HPLC columns (Phenomenex, Torrance, CA). Mobile phase A comprised 10 mM ammonium acetate (NH4Ac) and 0.015% formic acid in Milli-Q® water, and mobile phase B comprised 10 mM NH4Ac and 0.015% formic acid in acetonitrile:methanol:Milli-Q® water 65:30:5

(v/v/v). An API 4000 QTRAP (Applied Biosystems/MDS Sciex, Foster City, CA, USA) equipped with an electrospray ionization source was used for MS analysis. The 17 BAs were identified and quantified via the LC-MS/MS system (scheduled multiple reaction monitoring). The abundance of each BA was calculated from the area under the curve by normalizing to its respective isotope-labelled internal standard using Analyst® 1.5.2 software (Applied Biosystems/MDS Sciex). Calibration curves, quality controls, and samples were evaluated using MetIDQ™ software (BIOCRATES). Outliers were selected if more than 50% of the subjects were below the limit of detection. A heatmap view was generated using MetaboAnalyst; each concentration was transformed into log scale for visualization.

Metagenome analysis

To separate the extracellular vesicles (EVs) from human urine, EVs in urine samples were isolated using differential centrifugation at 10,000 × g for 10 min at 4 ℃. After centrifugation, bacteria and foreign particles were thoroughly eliminated by sterilizing the supernatant through a 0.22-μm filter. To extract the DNA out of the EV membrane, EVs separated from urine through previous steps were boiled for 40 min at 100 ℃. To eliminate remaining floating particles and waste, supernatant was collected after 30 min of centrifugation at 13,000 rpm at 4 ℃ and EV DNA was extracted using a PowerSoil DNA Isolation Kit (MO BIO Laboratories, Inc. Carlsbad, CA). The

standard protocol per the kit guide was followed. The DNA from the EVs in each sample was quantified by using QIAxpert system (QIAGEN, Germany).

Bacterial genomic DNA was amplified with 16S_V3_F (5′ -TCGTCGGCAGCGTCAGATGTGTATAAGAGACAGCCTACGGGNGGCWGCAG -3′) and 16S_V4_R (5′ -GTCTCGTGGGCTCGGAGATGTGTATAAGAGACAGGACTACHVGGGTATCTAATCC -3′) primers, which are specific for the V3-V4 hypervariable regions of 16S rDNA gene. The libraries were constructed using PCR products according to MiSeq System guide (Illumina, California, USA) and quantified using the QIAxpert system (QIAGEN). Each amplicon was then quantified and pooled at an equimolar ratio, and sequenced using the MiSeq system (Illumina) according to the manufacturer's recommendations.

Raw pyrosequencing reads obtained from the sequencer were filtered according to the barcode and primer sequences using the MiSeq system (Illumina). Taxonomic assignment was performed by profiling program MDx-Pro ver.1 (MD Healthcare, Korea). This program allows the selection of high-quality sequencing reads after checking the read length ($\geq$300 bp) and the quality score (average Phred score $\geq$20). Operational Taxonomy Units (OTUs) were clustered by using the sequence clustering algorithm CD-HIT. Subsequently, taxonomy assignment was carried out by using UCLUST and QIIME against the 16S rDNA sequence database in GreenGenes 8.15.13. Based on the sequence similarities, all 16S rDNA sequences were assigned to the following taxonomic levels. The bacterial composition at each level was plotted

as a stack bar. In case clusters could not be assigned at genus level due to lack of sequences or redundant sequences in the database, the taxon was assigned at a higher level, which is indicated in parenthesis.

Statistical analysis

For the data processing of LC-QTOFMS data, following the above data processing procedures, PCA was performed using the MPP software for both positive and negative ESI datasets, and showed sample clustering and distinguishing ions (filtered by $p < 0.05$, adjusted with false discovery rate [FDR] using the Benjamini and Hochberg method) between pre-dose and week 8.

Multivariate analysis of GC-TOFMS data and pathway analysis were conducted using Metaboanalyst 4.0. Normalized data sets were entered and principal components analysis (PCA) was performed to examine differentiation in overall metabolite profiles between groups. Pathway-associated metabolites were selected from an existing metabolite library and pathways with a Holm-corrected p-value and an FDR-adjusted p-value less than 0.05 were considered potential pathways mediated by UDCA.

Univariate analyses were performed using Graph Pad Prism version 7 (Graph Pad Software Inc., CA, USA) and SPSS 25.0 software (SPSS Inc., ILL, USA). For the comparison of paired samples, non-parametric equivalent Wilcoxon signed-ranks test was used. Repeat-measures ANOVA was conducted to compare group means with an equal number of sample points. p-values <0.05 were considered to indicate statistical significance.

RESULTS

PART I. Hepatoprotective effects of UDCA in healthy young subjects

Changes in LFT scores

To assess the hepatoprotective effect of drugs, serum parameters were analyzed in healthy subjects administered one of three different doses of UDCA (400, 800, or 1200 mg) for 2 weeks. As shown in Figure. 1A, ALT scores decreased following UDCA administration even in patients receiving low doses (400 mg). AST scores were also reduced in patients receiving 400 and 800 mg UDCA. However, no statistically significant change was observed for the 1200 mg group (Figure 1B). Further, circulating miR-122 levels was evaluated which is a potential biomarker of liver disease [18]. All three dosages of UDCA resulted in well controlled serum miR-122 levels (Figure 1C). These results indicate that UDCA administration resulted in diminished levels of the liver dysfunction biomarkers ALT, AST, and miR-122.

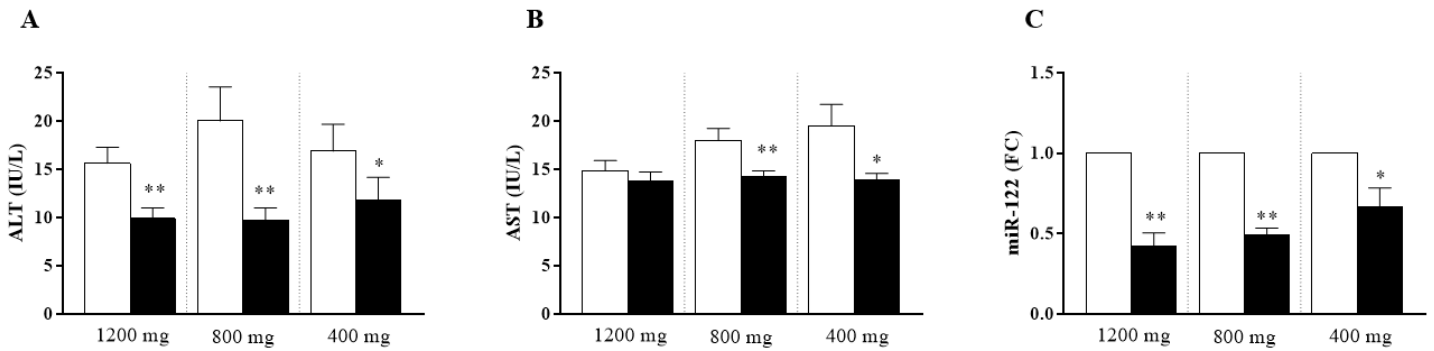

Figure 1. Changes in ALT, AST, and miR-122 levels after UDCA treatment. Bar graphs represent serum levels of (A) ALT, (B) AST, and (C) miR-122 before and after UDCA treatment (1200 mg, 800 mg, and 400 mg doses, respectively). White squares represent pre-dose levels; black squares, post-dose levels. The results are expressed as the mean ± SEM. Asterisks represent statistical significance (* represents p-value <0.05 and ** represents p-value <0.01) as determined via Wilcoxon signed-rank test between pre-dose and post-dose values. FC indicates fold change

Table 1. Liver function parameters measured in the serum before and after treatment.

Liver function parameters	1200 mg (n=8)			800 mg (n=8)			400 mg (n=8)		
	Pre-dose	**Post-dose**	**p-value**	**Pre-dose**	**Post-dose**	**p-value**	**Pre-dose**	**Post-dose**	**p-value**
Alanine aminotransferase (IU/L)	15.63 ± 1.65	9.88 ± 1.13	**	20.00 ± 3.56	9.75 ± 1.24	**	16.88 ± 2.81	11.75 ± 2.42	*
Aspartate aminotransferase (IU/L)	14.88 ± 1.03	13.75 ± 0.98	ns	18.00 ± 1.24	14.25 ± 0.59	**	19.50 ± 2.24	13.88 ± 1.96	*
miR-122 (fold change)	1.00 ± 0.00	0.42 ± 0.08	**	1.00 ± 0.00	0.50 ± 0.04	**	1.00 ± 0.00	0.67 ± 0.12	*

Data are the mean ± standard error of mean. Asterisks represent statistical significance (* represents p-value <0.05 and ** represents p-value <0.01) as determined via Wilcoxon signed-rank test. ns represents not significant

Bile acid profiling

A total of 15 bile acids, including primary and secondary bile acids, were measured in the plasma. Lithocholic acid (LCA) and taurolithocholic acid were excluded from analysis because their levels were below the detection limit. A heatmap was plotted by converting changes in bile acid concentrations, compared with their pre-dose concentrations, into a log scale (Figure 2-4). The plasma levels of bile acids, particularly UDCA and its conjugates, tauroursodeoxycholic acid (TUDCA) and glycoursodeoxycholic acid (GUDCA), were elevated at 2 week 8 of UDCA treatment for the three dosages (Figure 2-4). Interestingly, taurodeoxycholic acid (TDCA) was statistically significantly reduced upon UDCA 400 mg, 800 mg or 1200 mg (Figure 2H, Figure 3D and Figure 4F). In UDCA 1200 mg group, cholic acid (CA) were also increased after the treatment while glycodeoxycholoic acid (GDCA), taurocholic acid (TCA) and taurochenodeoxycholic acid (TCDCA) were reduced (Figure 2). In UDCA 400 mg group, glycocholic acid (GCA) and TCDCA reduced after 2 weeks of UDCA administration (Figure 4). In summary, UDCA only reduced hydrophobic bile acids, especially TDCA, in healthy young subjects

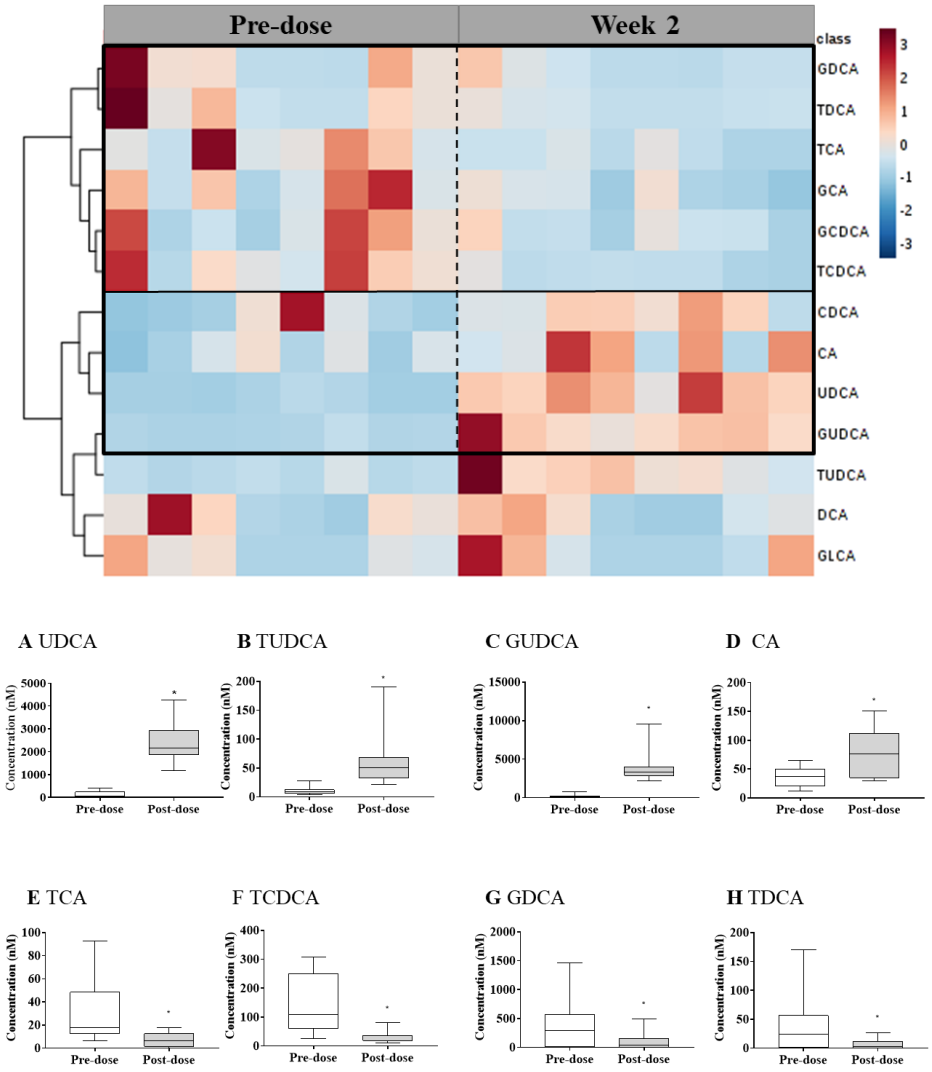

Figure 2. Heatmap and boxplots of bile acids that significantly changed after UDCA 1200 mg treatment. For the heatmap, the plasma concentration of each bile acid was converted to a log scale. Normalisation was carried out using the mean value of each bile acid. Heatmap shows the changes in bile acid levels from pre-dose to week 2 for UDCA treatment. The colour scale ranges from −3 (blue) to 3 (red). Dotted lines distinguish the clusters of bile acids showing distinct patterns after treatment compared with those at pre-dose. Boxplots

represent the concentrations (nM) of each bile acid: (A) UDCA, (B) TUDCA, (C) GUDCA, (D) CA, (E) TCA, (F) TCDCA, (G) GDCA and (H) TDCA. The boxplots show 5% and 95% confidence intervals. Wilcoxon signed-rank test was used for statistical evaluation. * represents p-value <0.05 between pre-dose and week 2

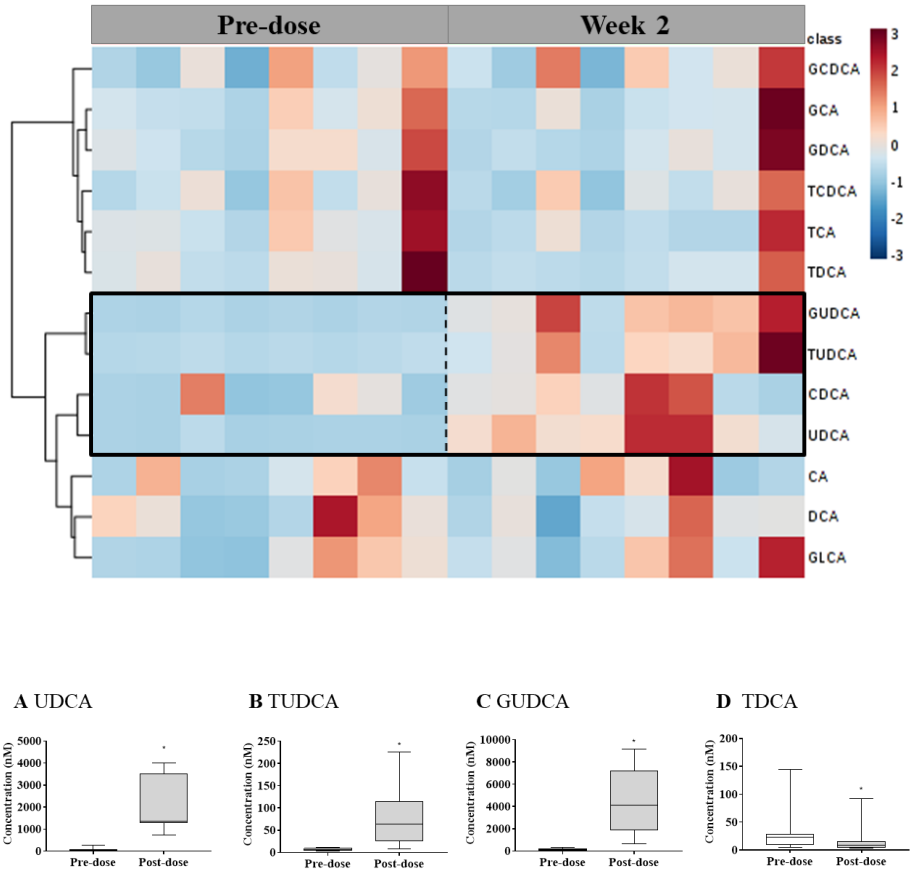

Figure 3. Heatmap and boxplots of bile acids that significantly changed after UDCA 800 mg treatment. For the heatmap, the plasma concentration of each bile acid was converted to a log scale. Normalisation was carried out using the mean value of each bile acid. Heatmap shows the changes in bile acid levels from pre-dose to week 2 for UDCA treatment. The colour scale ranges from −3 (blue) to 3 (red). Dotted lines distinguish the clusters of bile acids showing distinct patterns after treatment compared with those at pre-dose. Boxplots represent the concentrations (nM) of each bile acid: (A) UDCA, (B) TUDCA, (C) GUDCA, and (D) TDCA. The boxplots show 5% and 95% confidence intervals. Wilcoxon signed-rank test was used for statistical evaluation. *

represents p-value <0.05 between pre-dose and week 2

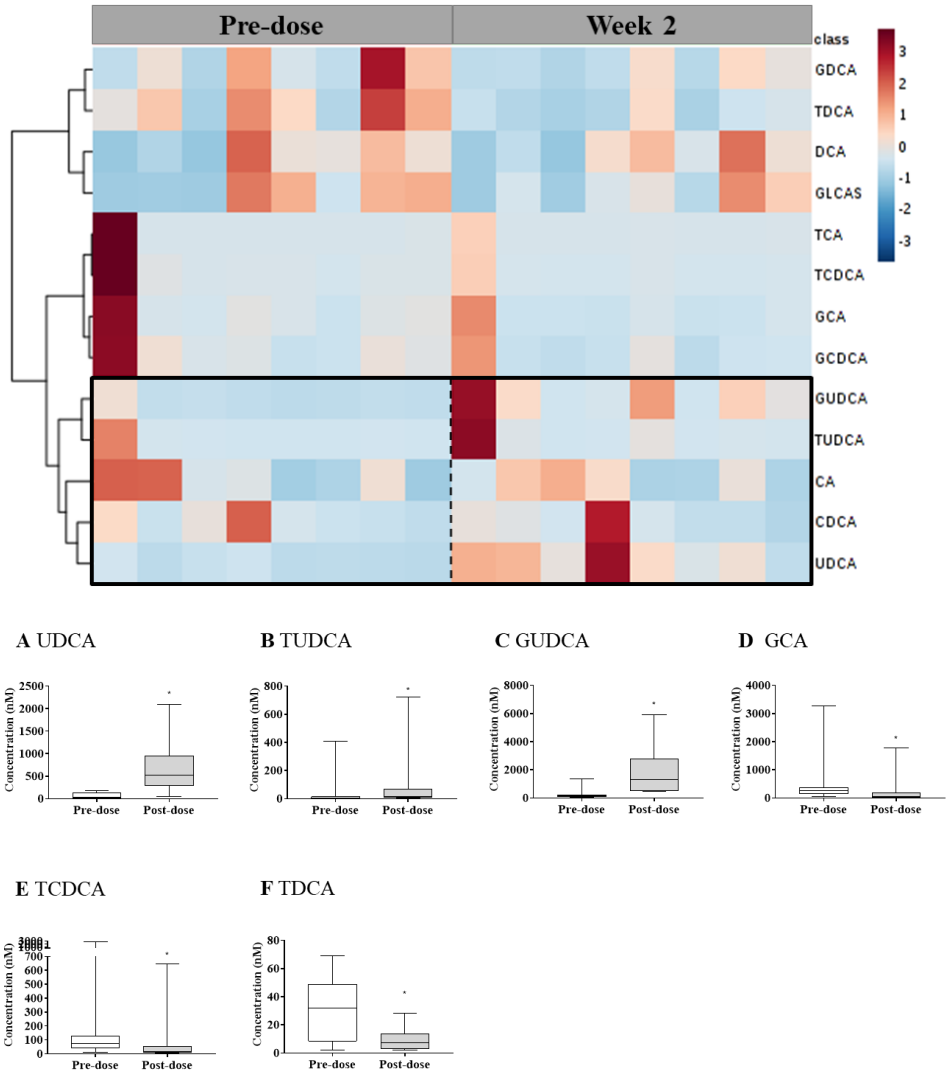

Figure 4. Heatmap and boxplots of bile acids that significantly changed after UDCA 400 mg treatment. For the heatmap, the plasma concentration of each bile acid was converted to a log scale. Normalisation was carried out using the mean value of each bile acid. Heatmap shows the changes in bile acid levels from pre-dose to week 2 for UDCA treatment. The colour scale ranges from −3 (blue) to 3 (red). Dotted lines distinguish the clusters of bile acids showing distinct patterns after treatment compared with those at pre-dose. Boxplots

represent the concentrations (nM) of each bile acid: (A) UDCA, (B) TUDCA, (C) GUDCA, (D) GCA, (E) TCDCA and (F) TDCA. The boxplots show 5% and 95% confidence intervals. A paired t-test was used for statistical evaluation. * represents p-value <0.05 between pre-dose and week 2

Metabolomic profiling via combined LC-QTOFMS and GC-TOFMS analysis

To assess systemic variations in small-molecule metabolites after drug treatment, Global metabolomics analysis was conducted using urine and plasma samples obtained before and after treatment with UDCA. Multivariate analysis was also performed to identify modulated metabolites in patients treated with 400 and 800 mg doses, but no models with acceptable predictability could be generated. As such, it was instead provided the relative intensities of metabolites which were consistently modulated post-treatment in the 400 and/or 800 mg treatment groups. As a result, PCA score plots revealed different metabolomic signatures before and after treatment of 1200 mg UDCA (Figure 5). Data for Figure 5A and 5B were obtained from urine samples and 5C and 5D from plasma samples. PCA score plots in Figure 5A and 5C were obtained from LC/QTOFMS and indicated different metabolome signatures upon UDCA treatment, with the overall accuracies of 22.9% and 25.5%, respectively. Figure 5B and 5D were obtained from GC/TOFMS and showed overall accuracies of 37.8% and 38.3%, respectively.

All the metabolites fulfilled the criteria for univariate analysis, less than 0.05 of FDR-adjusted P-value. Based on the criteria, 28 metabolites via LC-QTOFMS and 12 metabolites via GC-TOFMS were finally selected as potentially modulated by UDCA administration (Table 2-3). As shown in Figure 6 and Figure 7, box plots represent the relative intensity values of identified metabolites in urine and plasma, respectively. Interestingly, it was

observed several flavonoid compounds such as fertaric acid, ferulic acid-sulfate, and vanillin, which were elevated in urine samples (Figure 6 and Table 2-3). Further, phenylalanine metabolites such as phenylalanyl-alanine and polyphenylalanine were also reduced after treatment. Upon urine sample analysis, the levels of certain amino acids such as L-threonine, alanine, fumaric acid, lysine, and histidine were reduced after UDCA treatment (Figure 6). Similar patterns of metabolite alterations were observed in plasma samples, with a phenylalanine containing metabolite, glutamyl-phenylalanine, being decreased and the hydroxycinnamic acid containing metabolites p-hydroxyphenethyl trans-ferulate, cholesteryl ferulate, and cinnamyl alcohol presenting elevated levels (Figure 7). Moreover, the levels of some fatty acids were decreased following UDCA administration, including lysophosphatidylcholine (lyso-PC), and phosphoethanolamine (PE). Linoleic acid, however, was the only fatty acid induced by UDCA at the plasma level (Figure 7). Using GC/TOFMS analysis, glutamine and D-fructose were determined as metabolomics markers. Threonine levels were lower in plasma samples than in urine samples. Together, the data indicate that UDCA alters amino acid and fatty acid levels and increases levels of phenol-containing compounds in biological fluids. To assess the hepatoprotective effect of drugs, serum parameters were analyzed in healthy subjects administered one of three different doses of UDCA (400, 800, or 1200 mg) for 2 weeks.

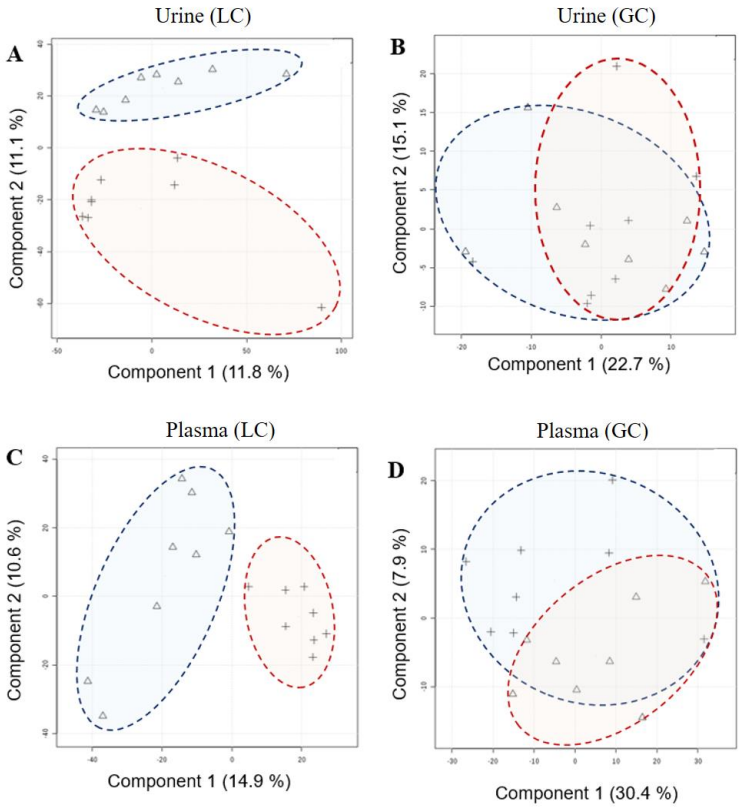

Figure 5. Score plots for principal component analysis (PCA). Score plots (A) and (B) represent data from urine samples acquired using liquid chromatography coupled with quadrupole-time-of-flight mass spectrometry (LC/QTOFMS) and gas chromatography-TOFMS (GC/TOFMS), respectively. Score plots (C) and (D) represent data from plasma samples acquired using LC/QTOFMS and GC/TOFMS, respectively. Pre-treatment samples are lined with blue; post-treatment samples, red

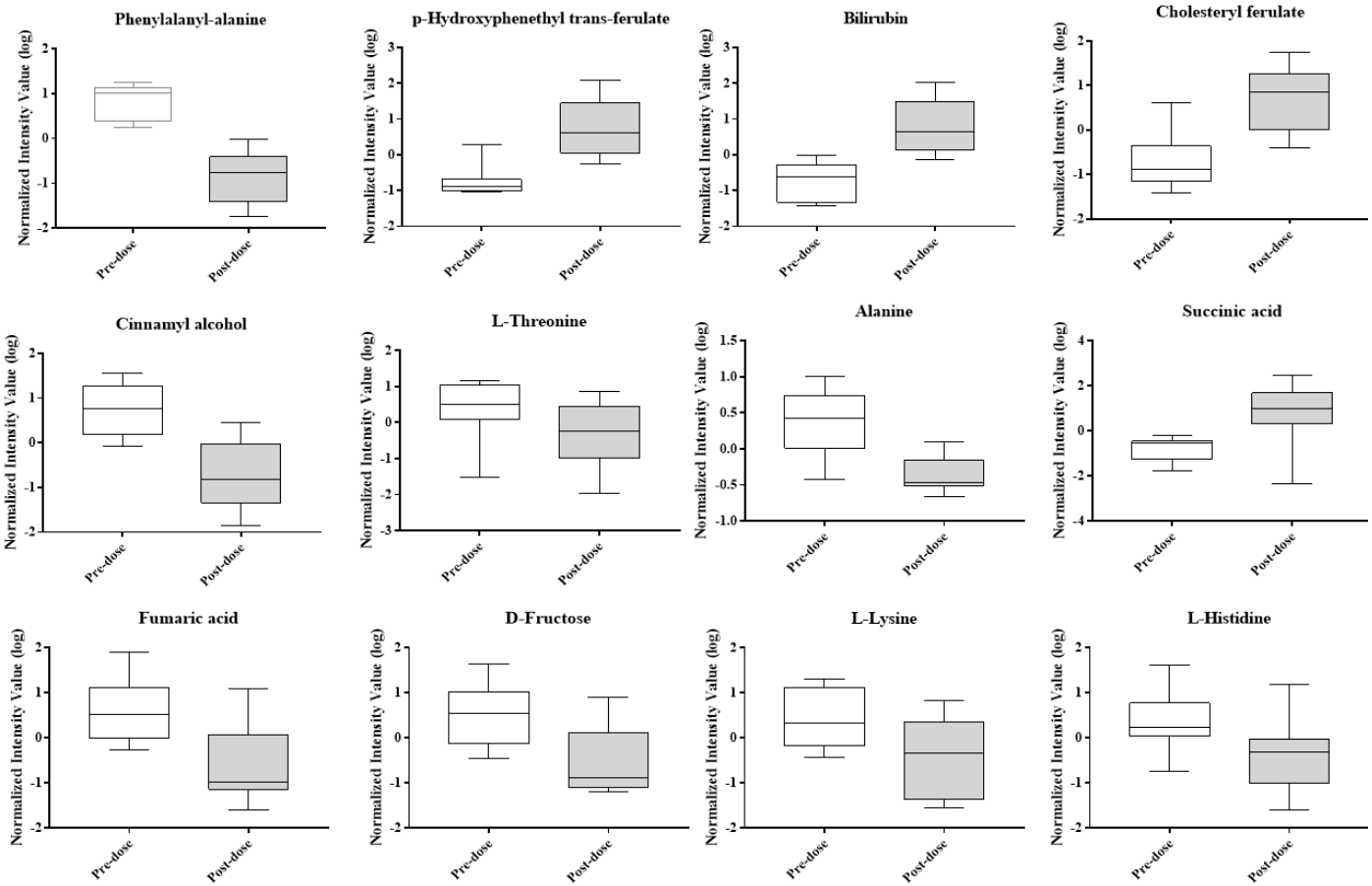
Phenylalanyl-alanine
p-Hydroxyphenethyl trans-ferulate
Bilirubin
Cholesteryl ferulate
Cinnamyl alcohol
L-Threonine
Alanine
Succinic acid
Fumaric acid
D-Fructose
L-Lysine
L-Histidine
Normalized Intensity Value (log)
Pre-dose
Post-dose

Figure 6. Relative intensity of identified metabolites in urine. Box plots represent relative intensities of identified metabolites in the urine. Representative urinary metabolites are phenylalanyl-alanine, fertaric acid, homovanillic acid sulfate, ferulic acid 4-sulfate, arginyl-asparagine, L-threonine, alanine, succinic acid, fumaric acid, D-fructose, L-lysine, and L-histidine. Box plots show 5% and 95% confidence intervals. White squares represent pre-dose levels; grey squares, post-dose levels. FDR-adjusted p-value <0.05 was used for statistical evaluation

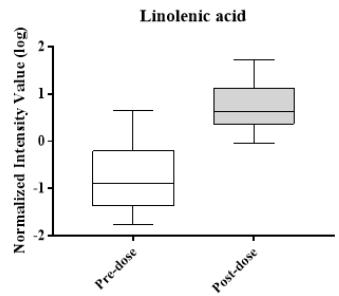
Linolenic acid
Normalized Intensity Value (log)
Pre-dose
Post-dose

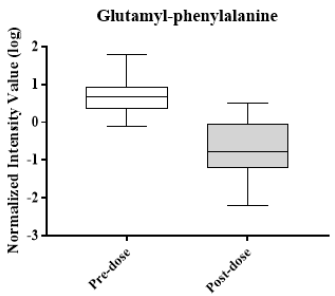
Glutamyl-phenylalanine
Normalized Intensity Value (log)
Pre-dose
Post-dose

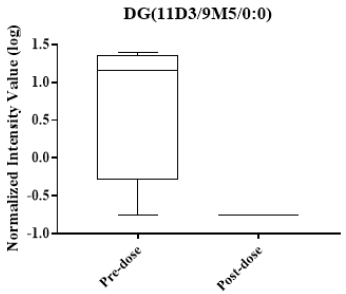
DG(11D3/9M5/0:0)
Normalized Intensity Value (log)
Pre-dose
Post-dose

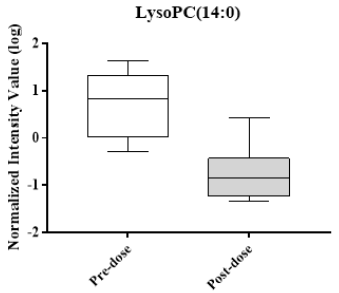
LysoPC(14:0)
Normalized Intensity Value (log)
Pre-dose
Post-dose

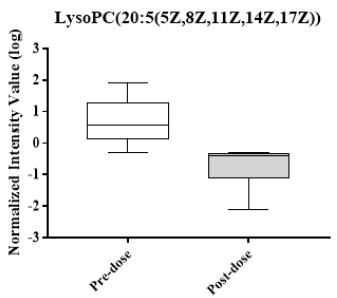
LysoPC(20:5(5Z,8Z,11Z,14Z,17Z))
Normalized Intensity Value (log)
Pre-dose
Post-dose

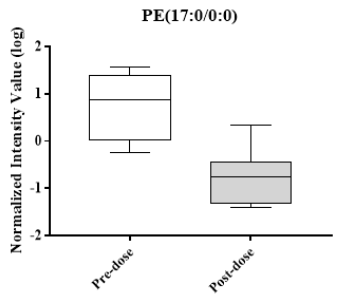
PE(17:0/0:0)
Normalized Intensity Value (log)
Pre-dose
Post-dose

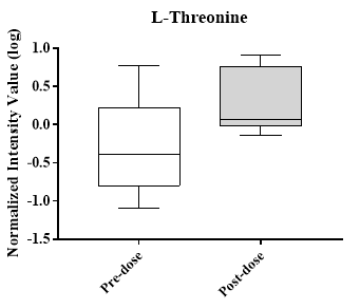
L-Threonine
Normalized Intensity Value (log)
Pre-dose
Post-dose

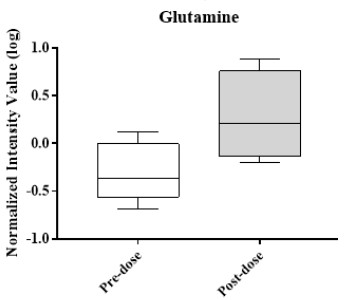
Glutamine
Normalized Intensity Value (log)
Pre-dose
Post-dose

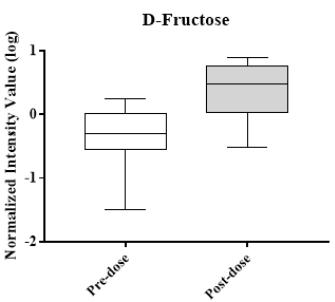
D-Fructose
Normalized Intensity Value (log)
Pre-dose
Post-dose

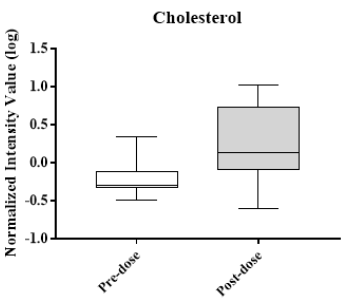
Cholesterol
Normalized Intensity Value (log)
Pre-dose
Post-dose

Figure 7. Relative intensity of identified plasma metabolites. Box plots represent the relative intensity of identified plasma metabolites, including linoleic acid, glutamy-phenylalanine, diacylglyceride, lysophosphatidylcholine, phosphoethanolamine, p-hydroxyphenethyl trans-ferulate, bilirubin, choesteryl ferulate, cinnamyl alcohol, L-threonine, glutamine, and D-fructose. Box plots show 5% and 95% confidence intervals. White squares represent pre-dose levels; grey squares, post-dose levels. FDR-adjusted p-value <0.05 was used for statistical evaluation

Table 2. Urine and plasma metabolites identified via liquid chromatography coupled with quadrupole-time-of-flight mass spectrometry analysis

tR min	Observed mass m/z	Parent molecule	Chemical Formula	Identity	Corrected p-value	VIP score	Sample	Level of MSI	HMDB ID	UDCA vs predose
5.6	154.0258	154.0266	C7H6O4	**2,4-Dihydroxybenzoic acid**	0.023	2.3	urine	1	HMDB0029666	2.8
8.0	222.0908	222.0892	C12H14O4	Vanillin isobutyrate	0.034	2.2	urine	2	HMDB0037681	2.7
5.2	236.1227	236.1161	C12H16N2O3	**Phenylalanyl-Alanine**	0.001	2.6	urine	1	HMDB0028988	-3.3
7.2	260.0320	259.9991	C9H8O7S	Caffeic acid sulfate	0.023	2.3	urine	1	HMDB0041706	2.8
6.0	262.0475	262.0147	C9H10O7S	Homovanillic acid sulfate	0.020	2.3	urine	1	HMDB0011719	2.8
7.0	262.1372	262.1317	C14H18N2O3	prolylphenylalanine	0.005	2.5	urine	2	HMDB0011179	-3.1
5.9	274.0470	274.0147	C10H10O7S	Ferulic acid 4-sulfate	0.047	2.2	urine	1	HMDB0029200	2.6
6.6	282.0283	282.0376	C12H10O8	2-O-Caffeoyltartronic acid	0.021	2.3	urine	2	HMDB0040869	2.8
5.9	288.1304	288.1313	C10H19N5O5	Arginyl-Asparagin	0.016	2.4	urine	2	HMDB0028704	-2.9
5.8	326.0792	326.0638	C14H14O9	Fertaric acid	0.036	2.2	urine	1	HMDB0029199	2.7
5.5	354.0346	354.0587	C15H14O10	2-O-p-Coumaroylhydroxycitric acid	0.037	2.2	urine	2	HMDB0040570	2.7
8.3	412.1989	412.1634	C22H24N2O6	Dicaffeoylputrescine	0.000	2.8	urine	2	HMDB0033467	3.4
12.4	464.2004	464.2046	C24H32O9	Estriol-3-glucuronide	0.024	2.3	urine	1	HMDB0010335	2.8
11.2	476.2688	476.2410	C26H36O8	Retinoyl glucuronide	0.001	2.6	urine	1	HMDB0010335	3.2
11.8	494.2318	494.2451	C25H38N2O6S	**Leukotriene D5**	0.025	2.3	urine	2	HMDB0014715	2.8

11.8	551.2441	551.2003	C26H33NO12	**Simmondsin 2'-ferulate**	0.014	2.4	urine	2	2994 HMDB0035475	2.9
10.8	650.3706	650.3819	C39H54O8	**23-trans-p-Coumaroyloxytormentic acid**	0.021	2.3	urine	2	HMDB0040682	2.8
0.7	238.0550	238.0630	C15H10O3	3-Hydroxyflavone	0.000	2.1	plasma	2	HMDB0031816	3.5
12.0	278.2201	278.2246	C18H30O2	Linolenic acid	0.001	1.8	plasma	1	HMDB0001388	2.9
12.5	308.2678	308.2715	C20H36O2	11,14-trans-Eicosadienoic acid	0.000	2.2	plasma	1	HMDB0005060	-3.0
8.3	314.1243	314.1154	C18H18O5	p-Hydroxyphenethyl trans-ferulate	0.001	2.1	plasma	2	HMDB0032806	2.7
12.1	354.2755	354.2770	C21H38O4	MG(0:0/18:2(9Z,12Z)/0:0)	0.000	1.3	plasma	2	HMDB0011538	-3.5
12.1	416.3276	416.3290	C27H44O3	Dihydroxycholest-5-en-26-al	0.001	1.5	plasma	2	HMDB0062736	2.8
12.2	467.3012	467.3012	C22H46NO7P	LysoPC(14:0/0:0)	0.000	2.1	plasma	2	HMDB0010379	-3.0
12.1	541.3161	541.3168	C28H48NO7P	LysoPC(20:5(5Z,8Z,11Z,14Z,17Z))	0.001	2.0	plasma	2	HMDB0010397	-2.7
9.3	584.2616	584.2635	C33H36N4O6	Bilirubin	0.001	2.1	plasma	1	HMDB0000054	2.8
14.7	663.4646	663.4839	C35H70NO8P	PE(14:0/16:0)	0.001	2.0	plasma	2	HMDB0008924	-2.9
14.8	729.5332	729.5309	C40H76NO8P	PC(14:0/18:2(9Z,12Z))	0.001	1.9	plasma	1	HMDB0007874	-2.7

NOTE: Bold type indicates metabolic markers that are significantly changed between 400 mg and 800 mg dose treatment groups

Table 3. Urine and plasma metabolites identified via gas chromatography-time-of-flight mass spectrometry analysis

tR sec	Unique mass m/z	Exact mass molecule	Similarity	Reverse	Probability	Identity	Corrected p-value	VIP score	Sample	Level of MSI	UDCA vs predose
415.6	218.0000	355.1768	923	923	9770	L-Threonine	0.015	1.3	urine	2	-1.5
431.0	248.0000	305.1663	885	896	8724	Alanine	0.003	1.0	urine	2	-1.3
510.2	292.0000	438.1745	801	936	9032	Succinic acid	0.025	1.6	urine	2	1.4
583.3	245.0000	260.1264	772	871	5826	Fumaric acid	0.002	1.4	urine	2	-2.1
737.6	217.0000	410.2160	910	914	3030	D-Fructose	0.003	1.6	urine	2	-1.9
586.5	96.0000	313.1642	873	873	8900	L-3-Methylhistidine	0.001	4.3	urine	2	-2.3
600.2	174.0000	434.2636	942	942	9844	L-Lysine	0.010	2.1	urine	2	-1.6
602.2	154.0000	371.1881	824	836	5154	L-Histidine	0.048	4.1	urine	2	-1.5
415.5	218.0000	335.1768	923	923	9765	L-Threonine	0.026	1.7	plasma	2	1.2
541.0	227.0000	434.2272	877	907	9694	L-Glutamine	0.027	1.8	plasma	2	1.2
588.9	217.0000	569.2876	920	920	3501	D-Fructose	0.037	1.6	plasma	2	1.3

NOTE: Bold type indicates metabolic markers that are significantly changed between 400 mg and 800 mg dose treatment groups

Pathway analysis of metabolite profiling data

To measure the centrality of a metabolite in a metabolic network, pathway topological analysis was performed using Metaboanalyst 4.0. All metabolites having Holm corrected and FDR adjusted p-values <0.05 were assessed for pathway analysis. As shown in Figure 8 and Table 4, the candidate pathways with an FDR-adjusted p-value <0.05 were 1) alanine, aspartate, and glutamate metabolism and 2) aminoacyl-tRNA biosynthesis. In addition, phenylalanine metabolism and tyrosine and histidine metabolism in the tricarboxylic acid (TCA) cycle also displayed p-values less than 0.05 but did not reach statistical significance upon FDR adjustment. Detailed statistical analysis is reported in Table 4. Further, it was proposed a network analysis with visualization, as shown in Figure 9. Web-based data from KEGG and HMDB were used for mapping. In conclusion, four major pathways were altered upon drug treatment: 1) amino acid metabolism, 2) flavonoid metabolism, 3) fatty acid metabolism and 4) the TCA

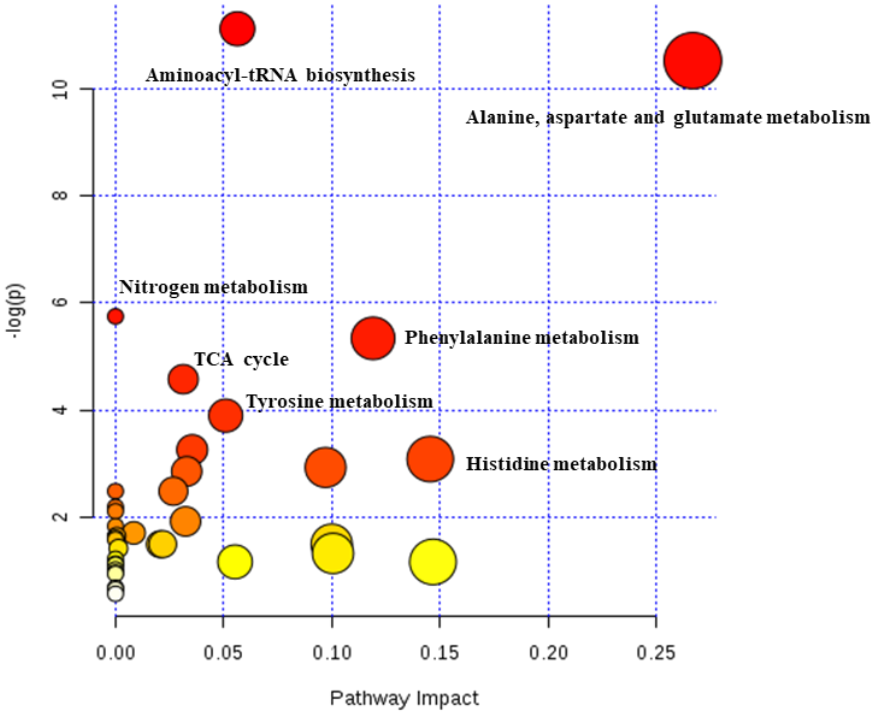

Figure 8. Analysis of metabolic pathways influenced by UDCA. A summary of pathway analysis representing the effect of identified metabolites on indicated pathways. The Y-axis represents the effect of the pathway and the X-axis presents a log scale of p-values. Metabolic pathways displaying statistical significance (FDR-adjusted p-value <0.001) were alanine, aspartate, and glutamate metabolism and aminoacyl-tRNA biosynthesis

Table 4. Statistical evaluation of pathway analysis

Pathway	Total	Expected	Hits	Raw p	Holm adjust	FDR	Impact
Aminoacyl-tRNA biosynthesis	75	0.592	6	0.000	0.001	0.001	0.056
Alanine, aspartate and glutamate metabolism	24	0.189	4	0.000	0.002	0.001	0.267
Nitrogen metabolism	39	0.308	3	0.003	0.249	0.085	0.000
Phenylalanine metabolism	45	0.355	3	0.005	0.370	0.096	0.119
Citrate cycle (TCA cycle)	20	0.158	2	0.010	0.783	0.165	0.031
Tyrosine metabolism	76	0.600	3	0.020	1.000	0.272	0.051
Butanoate metabolism	40	0.316	2	0.039	1.000	0.440	0.035
Histidine metabolism	44	0.347	2	0.046	1.000	0.459	0.145
Glycine, serine and threonine metabolism	48	0.379	2	0.054	1.000	0.462	0.097
Glyoxylate and dicarboxylate metabolism	50	0.395	2	0.058	1.000	0.462	0.033
Biotin metabolism	11	0.087	1	0.084	1.000	0.558	0.000
D-Glutamine and D-glutamate metabolism	11	0.087	1	0.084	1.000	0.558	0.027
Linoleic acid metabolism	15	0.118	1	0.112	1.000	0.692	0.000
Arginine and proline metabolism	77	0.608	2	0.122	1.000	0.696	0.000
Taurine and hypotaurine metabolism	20	0.158	1	0.147	1.000	0.751	0.032
Selenoamino acid metabolism	22	0.174	1	0.161	1.000	0.751	0.000
Steroid hormone biosynthesis	99	0.781	2	0.182	1.000	0.751	0.008
Valine, leucine and isoleucine biosynthesis	27	0.213	1	0.194	1.000	0.751	0.000
Phenylalanine, tyrosine and tryptophan biosynthesis	27	0.213	1	0.194	1.000	0.751	0.001
beta-Alanine metabolism	28	0.221	1	0.200	1.000	0.751	0.000
alpha-Linolenic acid metabolism	29	0.229	1	0.206	1.000	0.751	0.000
Glycerolipid metabolism	32	0.253	1	0.225	1.000	0.751	0.021
Pentose phosphate pathway	32	0.253	1	0.225	1.000	0.751	0.022
Lysine biosynthesis	32	0.253	1	0.225	1.000	0.751	0.100
Propanoate metabolism	35	0.276	1	0.244	1.000	0.780	0.001
Glycerophospholipid metabolism	39	0.308	1	0.268	1.000	0.824	0.101
Nicotinate and nicotinamide metabolism	44	0.347	1	0.297	1.000	0.851	0.000
Primary bile acid biosynthesis	47	0.371	1	0.313	1.000	0.851	0.055
Lysine degradation	47	0.371	1	0.313	1.000	0.851	0.147
Fatty acid biosynthesis	49	0.387	1	0.324	1.000	0.851	0.000
Starch and sucrose metabolism	50	0.395	1	0.330	1.000	0.851	0.000
Cysteine and methionine metabolism	56	0.442	1	0.362	1.000	0.904	0.000
Pyrimidine metabolism	60	0.474	1	0.382	1.000	0.923	0.000

Arachidonic acid metabolism	62	0.489	1	0.392	1.000	0.923	0.000
Amino sugar and nucleotide sugar metabolism	88	0.695	1	0.509	1.000	1.000	0.000
Purine metabolism	92	0.726	1	0.524	1.000	1.000	0.000
Porphyrin and chlorophyll metabolism	104	0.821	1	0.569	1.000	1.000	0.000

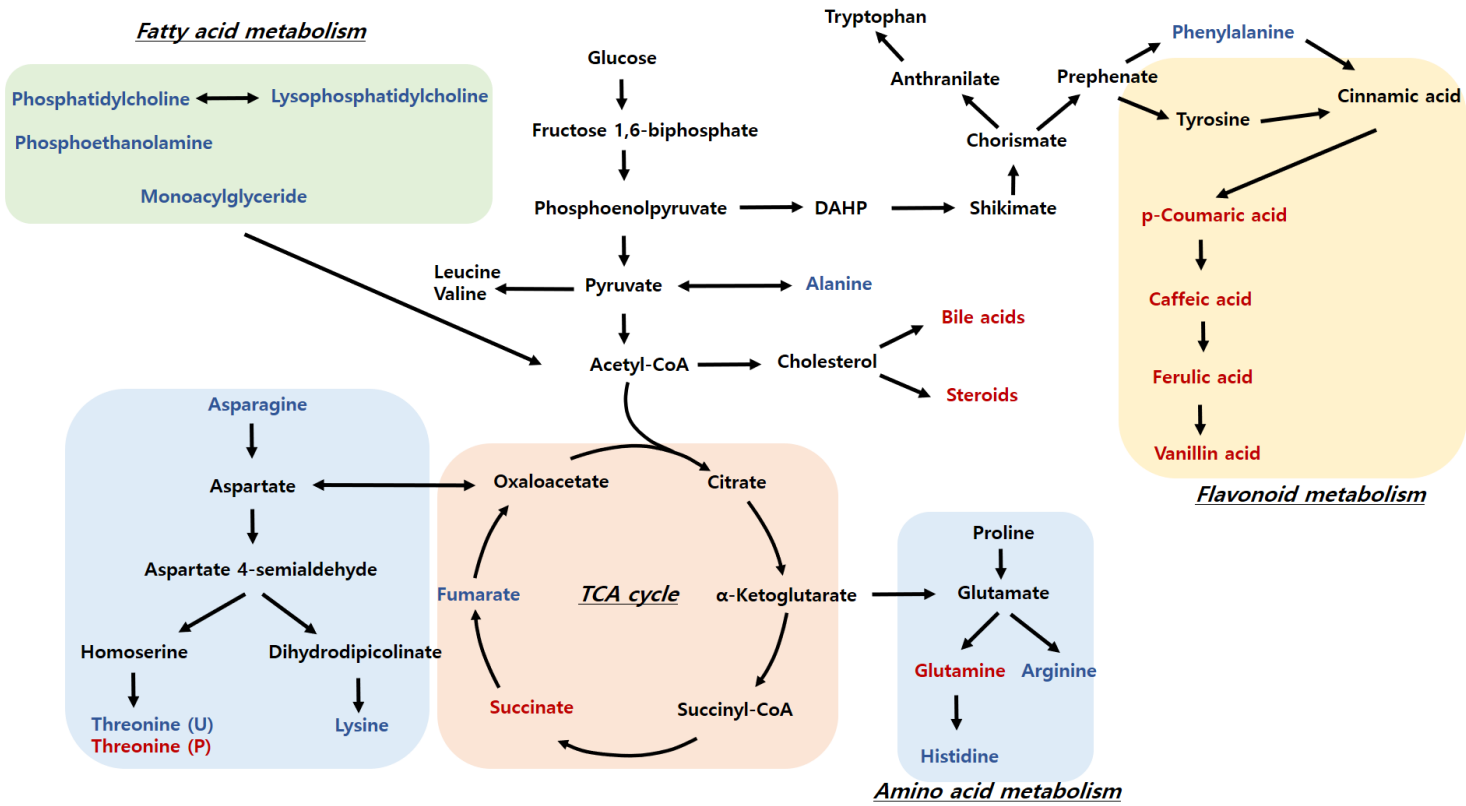
Fatty acid metabolism
Phosphatidylcholine
Lysophosphatidylcholine
Phosphoethanolamine
Monoacylglyceride
Glucose
Fructose 1,6-biphosphate
Phosphoenolpyruvate
DAHP
Shikimate
Chorismate
Tryptophan
Anthranilate
Prephenate
Phenylalanine
Tyrosine
Cinnamic acid
p-Coumaric acid
Caffeic acid
Ferulic acid
Vanillin acid
Flavonoid metabolism
Leucine
Valine
Pyruvate
Alanine
Acetyl-CoA
Cholesterol
Bile acids
Steroids
Asparagine
Aspartate
Aspartate 4-semialdehyde
Homoserine
Dihydrodipicolinate
Threonine (U)
Threonine (P)
Lysine
Oxaloacetate
Citrate
Fumarate
TCA cycle
α-Ketoglutarate
Succinate
Succinyl-CoA
Proline
Glutamate
Glutamine
Arginine
Histidine
Amino acid metabolism

Figure 9. A schematic representation of proposed pharmacological mechanisms of UDCA. Metabolomic profiling of urine and plasma samples revealed that UDCA regulates levels of amino acids such as phenylalanine, glutamine, arginine, alanine, histidine, lysine, and threonine, as well as metabolites including fumarate and succinate. Levels of phenolic compounds such as p-coumaric acid, caffeic acid, ferulic acid, and vanillin acid were also elevated. In addition, the effect on fatty acid metabolism (phosphoethanolamine, lysophosphatidylcholine, monoacylglycerides, and diacylglycerides) is also shown. Metabolites elevated after UDCA treatment are indicated in red, while those decreased after UDCA treatment are indicated in blue

PART II. Hepatoprotective effects of UDCA in elderly subjects
Changes in LFT scores

To assess the hepatoprotective effect of drugs, serum parameters were analyzed in elderly subjects administered one of two different doses of UDCA (400 or 800 mg) for 2 weeks. As shown in Figure 10A and Table 5, ALT scores decreased following UDCA administration even in patients receiving low doses (400 mg). AST scores were also reduced in patients receiving 400 and 800 mg UDCA. However, no statistically significant change was observed for the 1200 mg group (Figure 10B). Circulating miR-122 level, a potential biomarker of liver disease was further evaluated [18]. All three dosages of UDCA resulted in well controlled serum miR-122 levels (Figure 10C). These results indicate that UDCA administration resulted in diminished levels of the liver dysfunction biomarkers ALT, AST, and miR-122.

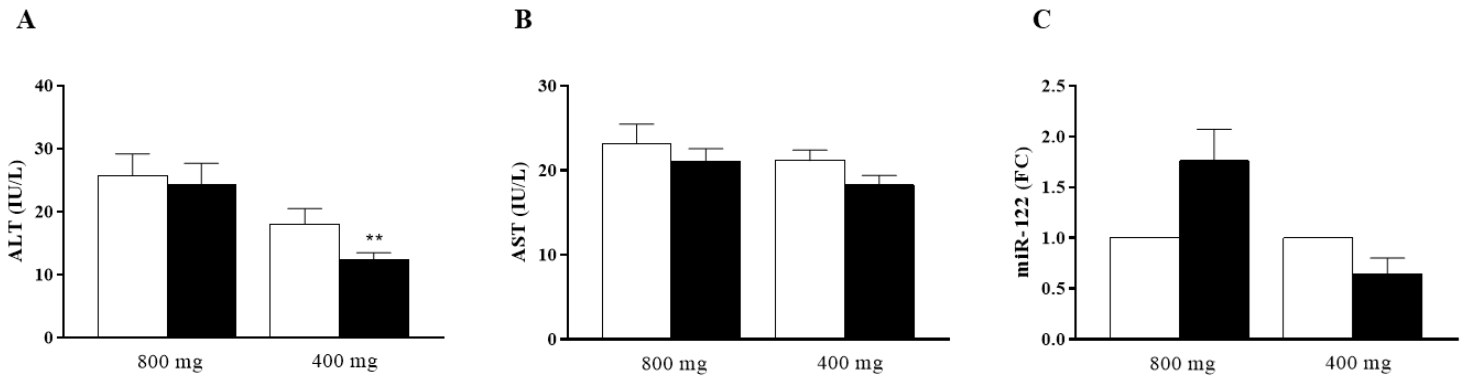

Figure 10. Changes in ALT, AST, and miR-122 levels after UDCA treatment. Bar graphs represent serum levels of (A) ALT, (B) AST, and (C) miR-122 before and after UDCA treatment (800 mg, and 400 mg doses, respectively). White squares represent pre-dose levels; black squares, post-dose levels. The results are expressed as the mean ± SEM. Asterisks represent statistical significance (* represents p-value <0.05 and ** represents p-value <0.01) as determined via Wilcoxon signed-rank test between pre-dose and post-dose values. FC indicates fold change

Table 5. Liver function parameters measured in the serum before and after treatment.

Liver function parameters	800 mg (n=8)			400 mg (n=8)		
	Pre-dose	**Post-dose**	**p-value**	**Pre-dose**	**Post-dose**	**p-value**
Alanine aminotransferase (IU/L)	25.75 ± 3.45	24.25 ± 3.44	ns	18.00 ± 2.47	12.38 ± 1.10	**
Aspartate aminotransferase (IU/L)	23.13 ± 2.33	21.00 ± 1.56	ns	21.13 ± 1.26	18.25 ± 1.15	ns
miR-122 (fold change)	1.00 ± 0.00	1.76 ± 0.31	ns	1.00 ± 0.00	0.64 ± 0.16	ns

Data are the mean ± standard error of mean. Asterisks represent statistical significance (* represents p-value <0.05 and ** represents p-value <0.01) as determined via Wilcoxon signed-rank test. ns represents not significant

Bile acid profiling

A total of 15 bile acids, including primary and secondary bile acids, were measured in the plasma. Lithocholic acid (LCA) and taurolithocholic acid were excluded from analysis because their levels were below the detection limit. A heatmap was plotted by converting changes in bile acid concentrations, compared with their pre-dose concentrations, into a log scale (Figure 11 and 12). The plasma levels of bile acids, particularly UDCA and its conjugates, tauroursodeoxycholic acid (TUDCA) and glycoursodeoxycholic acid (GUDCA), were elevated at 2 week of UDCA treatment for 800 and 400 mg group (Figure 11 and 12). Except for UDCA and its conjugates, there was no other bile acid species which are statistically significant. However, TCDCA and TDCA were reduced by UDCA treatment in similar to healthy subjects.

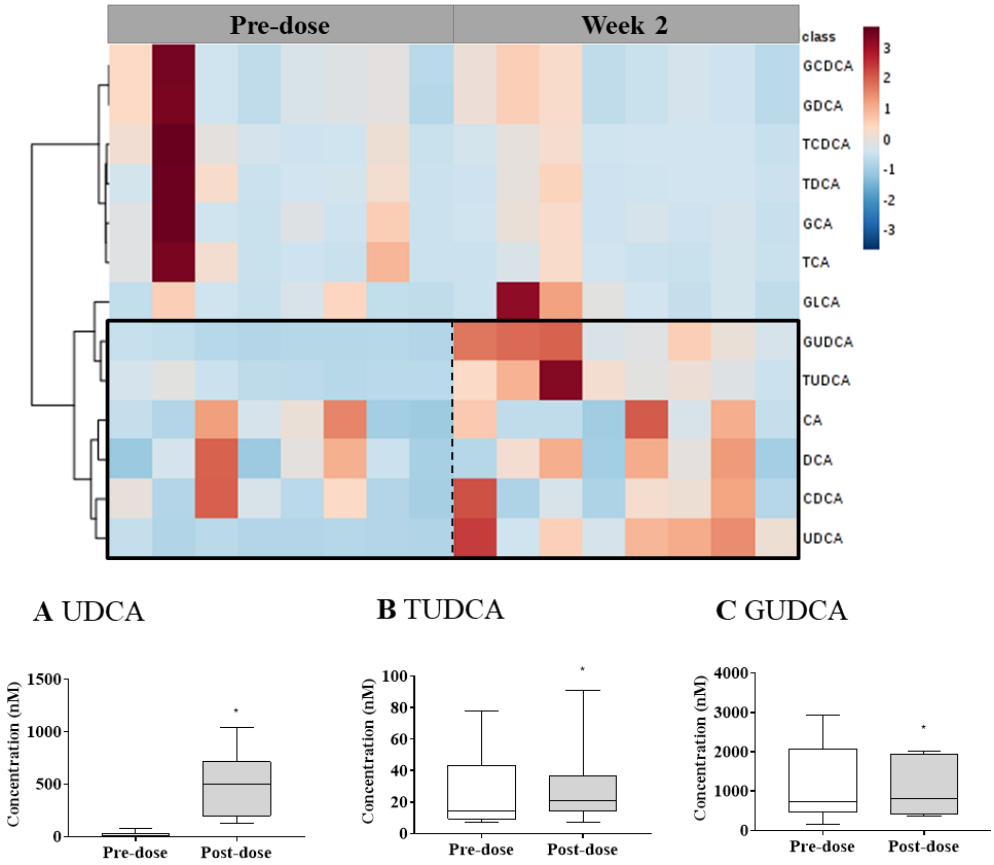

Figure 11. Heatmap and boxplots of bile acids that significantly changed after UDCA 800 mg treatment. For the heatmap, the plasma concentration of each bile acid was converted to a log scale. Normalisation was carried out using the mean value of each bile acid. Heatmap shows the changes in bile acid levels from pre-dose to week 2 for UDCA treatment. The colour scale ranges from −3 (blue) to 3 (red). Dotted lines distinguish the clusters of bile acids showing distinct patterns after treatment compared with those at pre-dose. Boxplots represent the concentrations (nM) of each bile acid: (A) UDCA, (B) TUDCA and (C) GUDCA. The boxplots show 5% and 95% confidence intervals. Wilcoxon signed-rank test was used for statistical evaluation. * represents p-value <0.05 between pre-dose and week 2

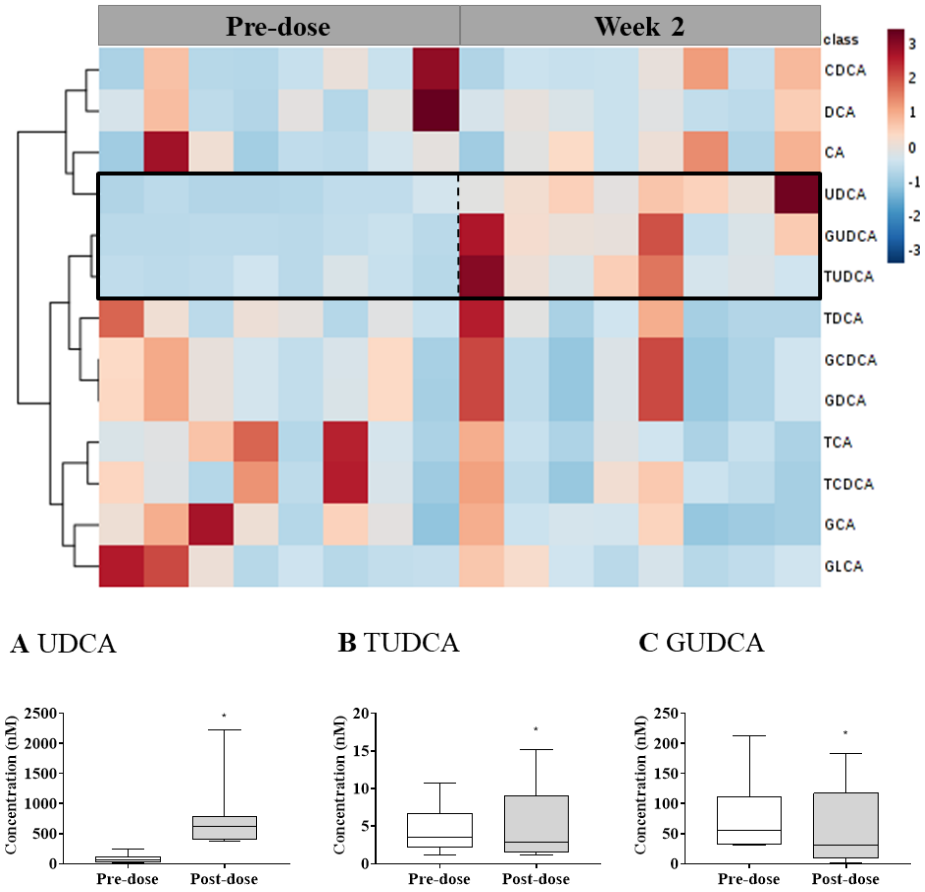

Figure 12. Heatmap and boxplots of bile acids that significantly changed after UDCA 400 mg treatment. For the heatmap, the plasma concentration of each bile acid was converted to a log scale. Normalisation was carried out using the mean value of each bile acid. Heatmap shows the changes in bile acid levels from pre-dose to week 2 for UDCA treatment. The colour scale ranges from −3 (blue) to 3 (red). Dotted lines distinguish the clusters of bile acids showing distinct patterns after treatment compared with those at pre-dose. Boxplots represent the concentrations (nM) of each bile acid: (A) UDCA, (B) TUDCA and (C) GUDCA. The boxplots show 5% and 95% confidence intervals.

Wilcoxon signed-rank test was used for statistical evaluation. * represents p-value <0.05 between pre-dose and week 2

PART III. Hepatoprotective effects of UDCA in patients with liver dysfunction

Changes in LFT scores

Flow chart of this study is shown in Figure 13. To determine the efficacy of the drugs, liver function parameters were measured in the serum, and the results for each group are listed in Figure 14 and Table 6. Compared with their baseline values, the alanine aminotransferase (ALT), aspartate aminotransferase (AST), and gamma-glutamyl transferase (GGT) levels were reduced by 40.3%, 33.9%, and 23%, respectively, after 4 weeks of UDCA treatment. Reduced levels were maintained at week 8, but the difference with the baseline was only significant for GGT, probably because of variations associated with the small sample size. Vitamin E treatment was also effective in improving the ALT and AST levels at both week 4 and week 8, while the GGT level was only reduced at week 8.

Circulating miR-122 is considered a potential biomarker for liver disease. It is the most frequently detected miRNA in the adult liver, accounting for approximately 70% of the total liver miRNA population and controlling liver-enriched transcription factors, including hepatocyte nuclear factor-4α and p53, thereby maintaining the proper balance between proliferation and differentiation of hepatocytes. It has been reported that miR-122 is upregulated in patients with hepatitis C and NAFLD.

Consistent with previous studies, the miR-122 level was significantly reduced by UDCA treatment (Figure 14D and Table 6), by 39% at week 4 and by 42% at week 8. These results suggested that UDCA might protect hepatocytes by

suppressing miR-122. Interestingly, vitamin E did not significantly reduce the miR-122 level at both time points, probably because outliers were not excluded. At week 8, one subject in the vitamin E group had an approximately two-fold higher level of miR-122 than those at pre-dose and week 4, and another subject had a more than three-fold higher miR-122 level at week 8 (data not shown). Nevertheless, vitamin E treatment was also effective in reducing liver dysfunction (Table 6).

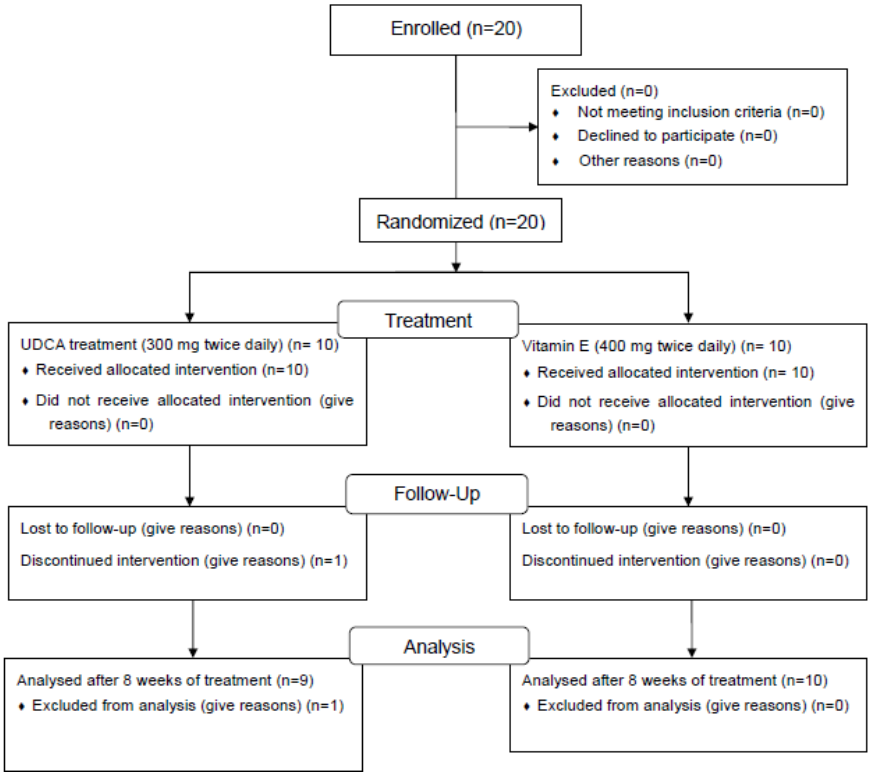

Figure 13. Flow chart of the study. A total of 20 subjects were enrolled in this study and underwent randomisation. Ten of them were assigned to take UDCA (300 mg twice daily), and the other 10 were treated with vitamin E (400 IU twice daily) for 8 weeks. During this period, one subject withdrew from the UDCA group for a personal reason after 4 weeks and therefore, was excluded from data analysis. The total number of subjects included in the final analysis was nine for the UDCA group and 10 for the vitamin E group

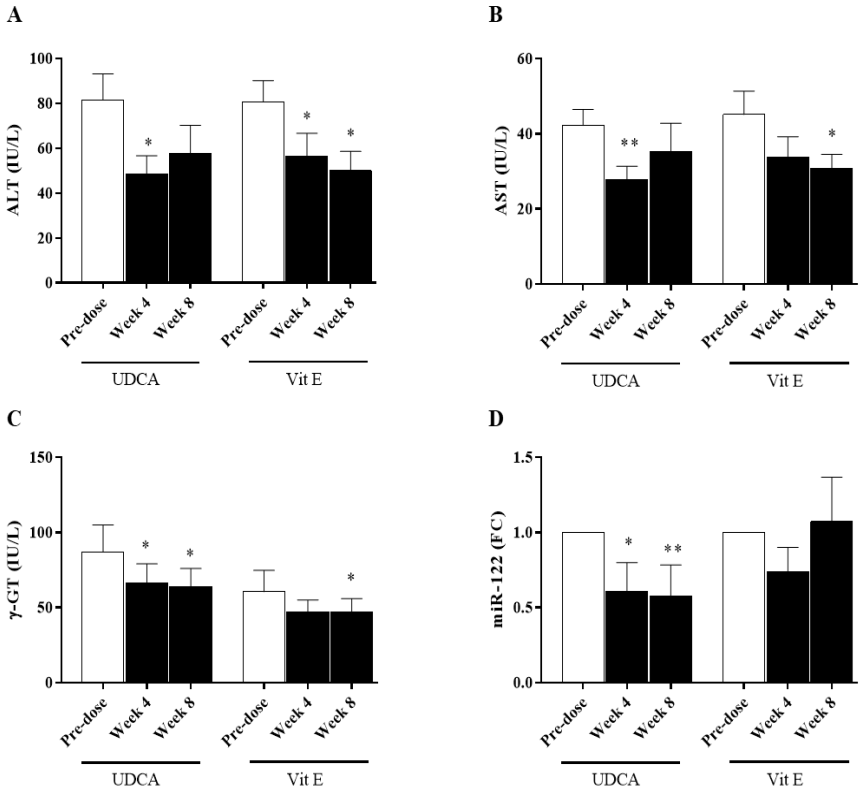

Figure 14. Changes in ALT, AST, γ-GT and miR-122 levels after UDCA treatment. Bar graphs represent serum levels of (A) ALT, (B) AST, (C) γ-GT and (D) miR-122 upon UDCA or Vit E treatment at pre-dose, week 4 and week 8. White squares represent pre-dose levels; black squares, post-dose levels of week 4 and week 8. The results are expressed as the mean ± SEM. Asterisks represent statistical significance (* represents p-value <0.05 and ** represents p-value <0.01) as determined via Wilcoxon signed-rank test. FC indicates fold change

Table 6. Liver function parameters measured in the serum before and after treatment.

Liver function parameters	UDCA (n=9)				Vitamin E (n=10)			
	Pre-dose	Week 4	Week 8	p-value	Pre-dose	Week 4	Week 8	p-value
Alanine aminotransferase (IU/L)	81.56 ± 11.63	48.67 ± 8.07	57.67 ± 12.56	†	80.7 ± 9.5	56.6 ± 10.1	50 ± 9	†, ‡
Aspartate aminotransferase (IU/L)	42.22 ± 4.24	27.89 ± 3.49	35.22 ± 7.59	†	45.1 ± 6.3	33.7 ± 5.5	30.9 ± 3.6	‡
Gamma-glutamyl transferase (IU/L)	87 ± 18	66.56 ± 12.59	64.11 ± 12.01	†, ‡	60.6 ± 14.2	47.1 ± 7.9	47.1 ± 9.0	‡
miR-122 (fold change)	1.00 ± 0.00	0.6078 ± 0.5740	0.5733 ± 0.633	†, ‡	1.00 ± 0.00	0.738 ± 0.514	1.073 ± 0.933	ns

Data are the mean ± standard error of mean. Wilcoxon signed-rank test was performed. † represents p-value <0.05 between pre-dose and week 4; ‡ represents p-value <0.05 between pre-dose and week 8. ns, not significant

Bile acid profiling

A total of 15 bile acids, including primary and secondary bile acids, were measured in the plasma. Lithocholic acid (LCA) and taurolithocholic acid were excluded from analysis because their levels were below the detection limit. A heatmap was plotted by converting changes in bile acid concentrations, compared with their pre-dose concentrations, into a log scale (Figure 15A and 15B). The plasma levels of bile acids, particularly UDCA and its conjugates, tauroursodeoxycholic acid (TUDCA) and glycoursodeoxycholic acid (GUDCA), were elevated at weeks 4 and 8 of UDCA treatment (Figure 15D and E). The level of deoxycholic acid (DCA) was statistically significantly reduced (Figure 15F). The decreases in the levels of DCA conjugates (glycodeoxycholic acid and taurodeoxycholic acid) and glycolithocholic acid were not significant. Raw values of concentrations (non-scaled values) were used for statistical comparisons. After vitamin E treatment, none of the bile acid levels changed during the study. There was no exclusion of outliers nor any correction for baseline levels across all the subjects because of the small sample size. In summary, UDCA only reduced hydrophobic bile acids, especially DCA, in subjects with liver dysfunction.

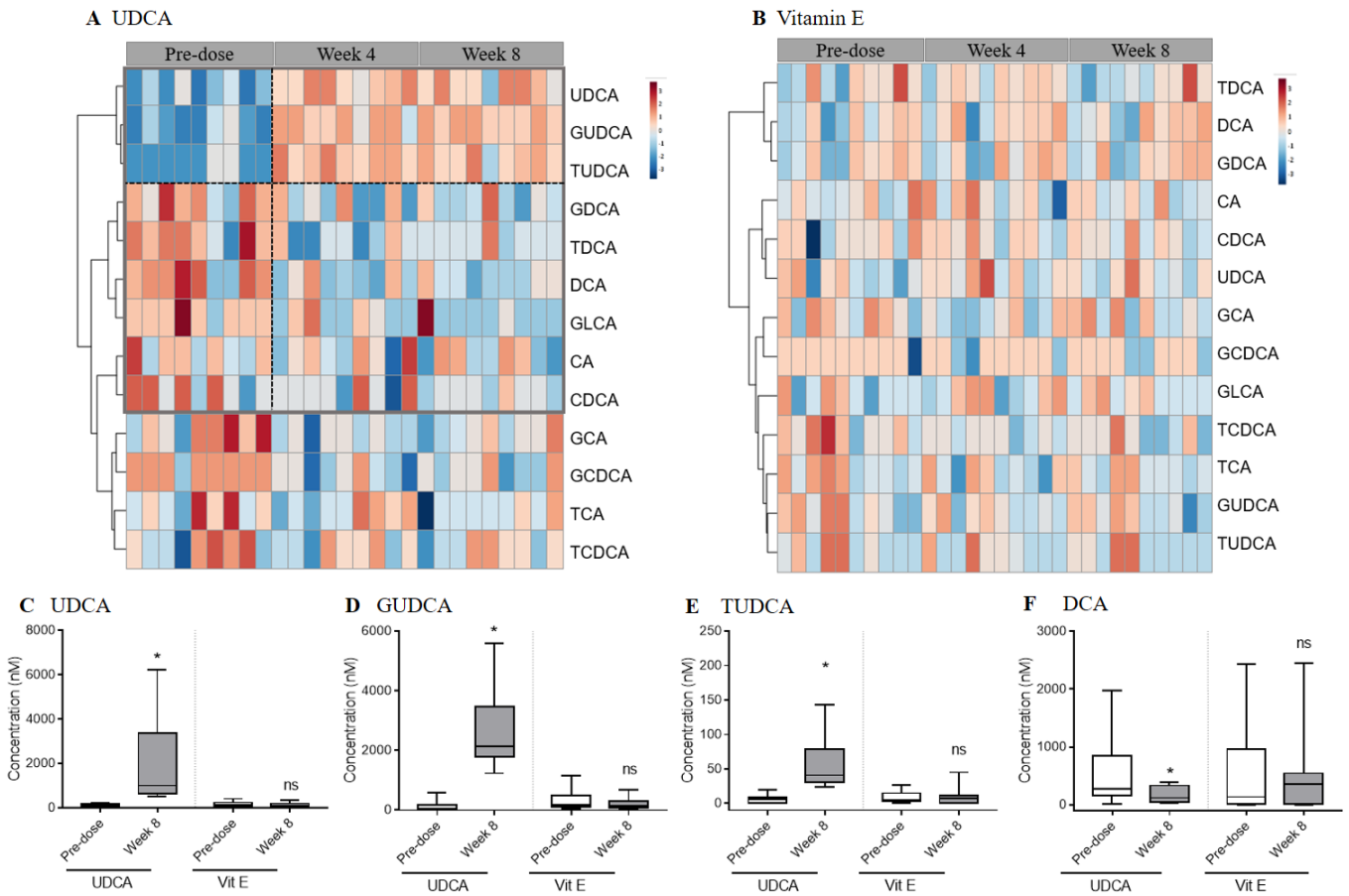
A UDCA
Pre-dose
Week 4
Week 8
UDCA
GUDCA
TUDCA
GDCA
TDCA
DCA
GLCA
CA
CDCA
GCA
GCDCA
TCA
TCDCA
B Vitamin E
Pre-dose
Week 4
Week 8
TDCA
DCA
GDCA
CA
CDCA
UDCA
GCA
GCDCA
GLCA
TCDCA
TCA
GUDCA
TUDCA
C UDCA
D GUDCA
E TUDCA
F DCA
Concentration (nM)
Pre-dose
Week 8
UDCA
Vit E
*
ns

Figure 15. Heatmaps and boxplots of bile acids that significantly changed after treatment. For heatmaps, the plasma concentration of each bile acid was converted to a log scale. Normalisation was carried out using the mean value of each bile acid. Heatmaps show changes in bile acid levels from pre-dose to week 4 and week 8 for (A) UDCA and (B) Vitamin E treatments. The colour scale ranges from −3 (blue) to 3 (red). Dotted lines distinguish the clusters of bile acids showing distinct patterns after treatment compared with those at pre-dose. Boxplots represent the concentrations (nM) of each bile acid: (C) UDCA, (D) GUDCA, (E) TUDCA, and (F) DCA. The boxplots show 5% and 95% confidence intervals. Wilcoxon signed-rank test was used for statistical evaluation. * represents p-value <0.05 between pre-dose and week 8; ns, non-significant difference between the groups

Global metabolomics profiling using LC-QTOFMS

To assess systemically changed small-molecule metabolites after each drug treatment, global metabolomic analysis was performed. The volcano plots presented in Figure 16 show the most significant metabolites found by univariate analysis. Three-dimensional principal component analysis (PCA) score plots showed clear differences between the two time points of each treatment. For example, Figure 16A demonstrates that the red spheres (week 8) were separated from the blue spheres (pre-dose), showing different metabolome signatures between the groups, with the overall accuracies of 55.1% for urine samples (Figure 16A) and 36.9% for plasma samples (Figure 16C) in the UDCA group. Metabolomic profiling also revealed a clear distinction between pre-dose and post-dose values after vitamin E treatment, with the overall accuracies of 40.1% in the urine (Figure 16B) and 40.8% in the plasma (Figure 16D).

A UDCA (Urine)

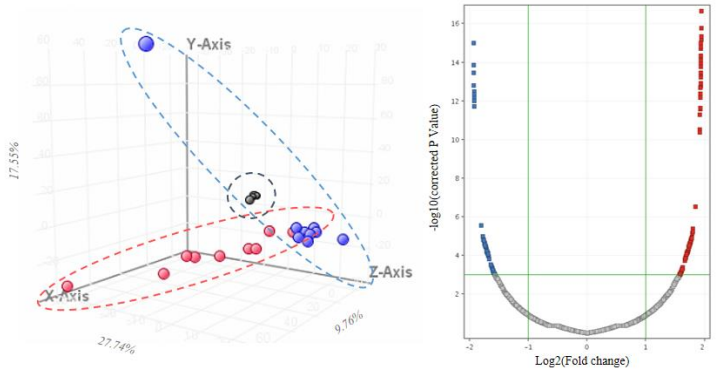

B Vitamin E (Urine)

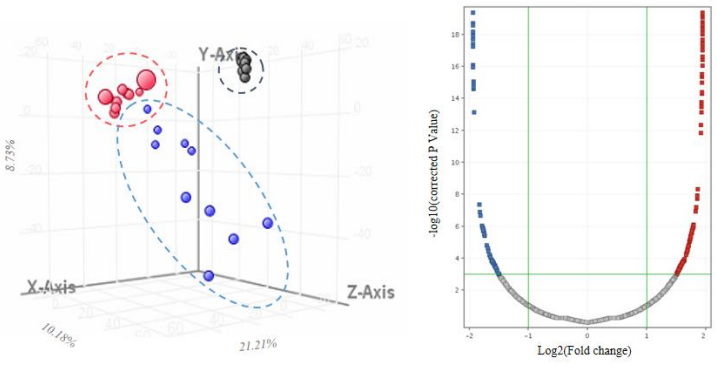

C UDCA (Plasma)

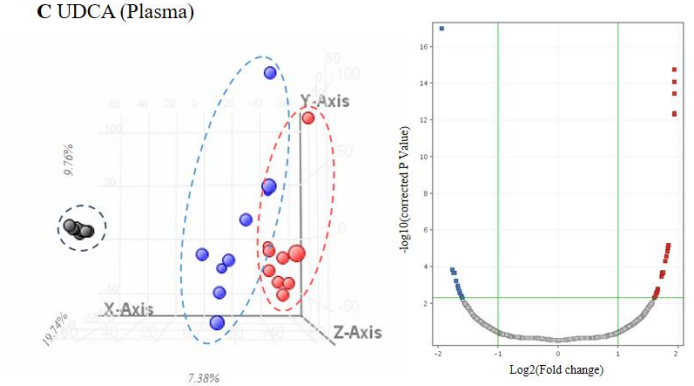

D Vitamin E (Plasma)

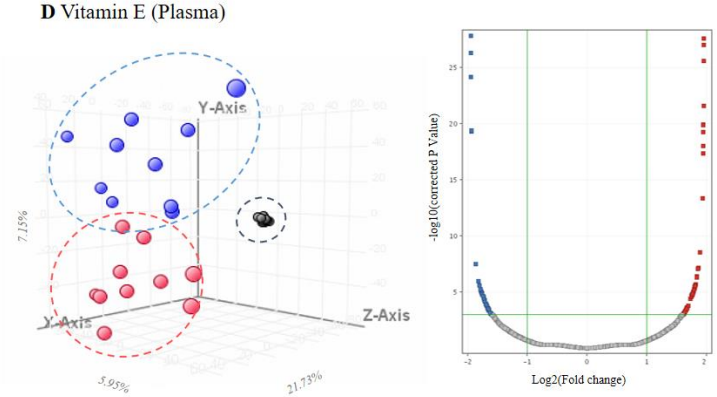

Figure 16. Estimation of urinary and plasma metabolites after UDCA and vitamin E treatments via global metabolomic analysis. Three-dimensional PCA data and volcano plots are shown for urine samples of (A) UDCA- and (B) vitamin E-treated patients and plasma samples of (C) UDCA- and (D) vitamin E-treated patients. In the PCA plot, blue and red spheres indicate pre-dose and week 8 samples, respectively. Black spheres represent the quality control sample used to verify the reproducibility and accuracy of the data. Each dotted circle indicates a cluster of spheres with the same colour. Values in the volcano plots show the metabolites that significantly changed, as found by multivariate analysis. Red squares indicate metabolites upregulated after treatment, and blue squares indicate metabolites downregulated after treatment

UDCA and vitamin E changed aromatic amino acids and their metabolites. The metabolites identified by multivariate analysis were selected according to their Q-values, which are P-values adjusted for the false discovery rate (FDR). The metabolites that showed statistical significance ($q < 0.05$) are listed in Table 7 and Table 8. Figure 17 shows the most frequent small-molecule metabolites produced via the phenylalanine/tyrosine or tryptophan pathway. Typically, as shown in Figure 17, L-phenylalanine and its downstream molecules, such as phenylacetic acid and homogentisic acid, were significantly reduced by UDCA. On the contrary, the level of a tryptophan metabolite, N-acetyltryptophan, increased. The level of 6-hydroxyindole decreased, and its glucuronidation increased. These data suggest that UDCA reduces systemic indole levels via hydroxylation and glucuronidation. In contrast, vitamin E treatment did not markedly reduce the levels of phenylalanine or indole-derived compounds, except 5-hydroxy-6-methoxyindole glucuronide. Further, induction of BAA-derived metabolites, acetyl-DL-valine and vanillic acid sulphate, supported the hypothesis that UDCA regulates AAAs and BAAs in liver dysfunction.

UDCA and vitamin E regulated uremic toxins and antioxidants. Uremic toxins such as hippuric acid and p-cresol are also products of the phenylalanine/tyrosine pathway, and their levels were well controlled by UDCA (Figure 17). Vitamin E only regulated the levels of tryptophan-derived metabolites, indoxyl sulphuric acid and 3-(3-indolyl)-2-oxopropanoic acid. This indicates that UDCA and vitamin E act via distinct mechanisms to exert

hepatoprotection. In addition, UDCA upregulated the antioxidants, N-acetyl-L-cysteine and ascorbate sulphate, and downregulated the oxidative stressors, 3-nitro-L-tyrosine and 4-hydroxynonenal glutathione (4-HNE GSH). Vitamin E significantly increased the ascorbate sulphate content and decreased inflammatory lipids such as 3-ketosphingosine and sphingosine. Using global metabolomic analysis, it was estimated that a number of metabolites with toxic effects or derived from the phenylalanine/tyrosine pathway were less likely to be affected by vitamin E. However, UDCA alleviated the metabolic changes associated with the phenylalanine, tyrosine, and tryptophan pathways and increased the levels of antioxidants in patients with liver dysfunction.

A Aromatic amino acid and branched-amino acid containing metabolites

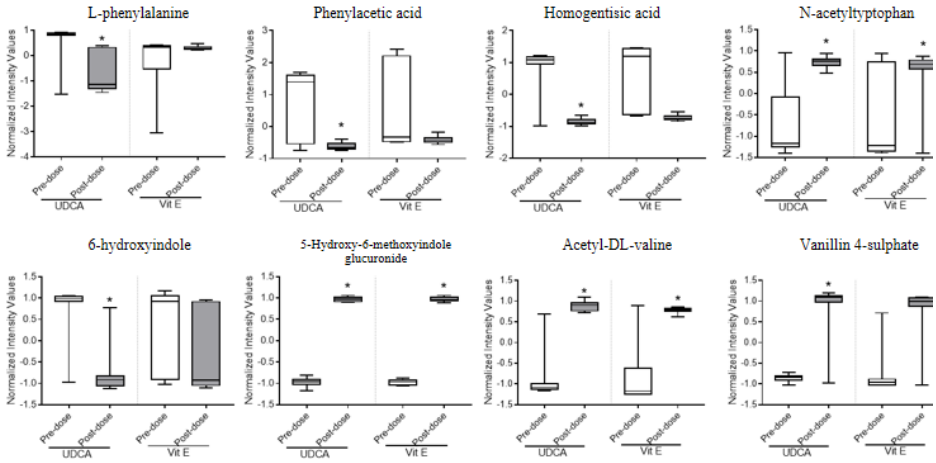

B Uremic toxins and anti-oxidants

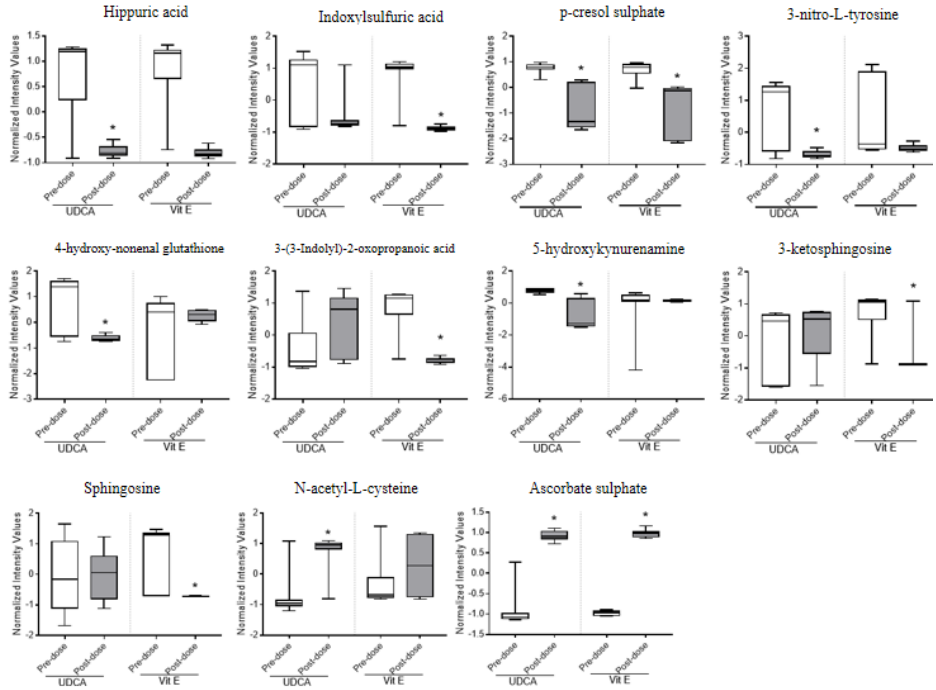

Figure 17. Relative intensity of identified metabolites. Relative intensities of each identified metabolite in the urine and plasma are shown with boxplots. (A) Metabolites containing aromatic amino acids or branched amino acids (L-phenylalanine, phenylacetic acid, homogentisic acid, N-acetyltryptophan, 6-hydroxyindole, 5-hydroxy-6-methoxyindole glucuronide, acetyl-DL-valine, and vanillic acid sulphate). (B) Metabolites known to be toxic [hippuric acid, indoxyl sulphuric acid, p-cresol sulphate, 3-nitro-L-tyrosine, 4-hydroxynonenal glutathione, 3-(3-indolyl)-2-oxopropanoic acid, 5-hydroxykynurenamine, 3-ketosphingosine, and sphingosine] or antioxidants (N-acetyl-L-cysteine and ascorbate sulphate). The boxplots show 5% and 95% confidence intervals. Wilcoxon signed-rank test was used for statistical evaluation. * represents FDR-adjusted p-value <0.05 between pre-dose and week 8

Table 7. Urinary metabolites identified by global metabolomic analysis in a negative ESI mode.

tR (min)	Mass (*m/z*)	Delta Da	Chemical formula	Identity	q-value	Identification	UDCA vs pre-dose	Vit E vs pre-dose
0.71	197.0722	−0.0034	$C_9H_{11}NO_4$	3-(3,4-Dihydroxyphenyl)-DL-alanine	0.0216	MS/MS	2.65	
1.06	233.0329	0.0029	$C_8H_{11}NO_5S$	Dopamine 3-*O*-sulphate	0.0216	MS/MS		−2.69
1.15	255.9875	0.0014	$C_6H_8O_9S$	Ascorbate sulphate	0.0216	MS/MS	3.58	3.78
1.47	165.062	0.017	$C_9H_{11}NO_2$	L-Phenylalanine	0.0216	MS/MS	−2.27	
1.84	168.0372	0.0051	$C_8H_8O_4$	Homogentisic acid	0.0216	MS/MS	−3.26	
2.06	226.0916	−0.0326	$C_9H_{10}N_2O_5$	3-Nitro-L-tyrosine	0.0256	MS/MS	−2.60	
2.36	169.0355	0.002	$C_7H_7NO_4$	Dihydrodipicolinic acid	0.0228	Database		3.81
2.82	154.0279	−0.0013	$C_7H_6O_4$	2,4-Dihydroxybenzoic acid	0.0216	MS/MS	2.96	3.45
3.58	194.0654	0.0037	$C_9H_{10}N_2O_3$	Aminohippuric acid	0.0228	Database		−2.76
3.63	173.9963	0.0024	$C_6H_6O_4S$	4-Hydroxybenzenesulphonic acid	0.0216	MS/MS	−3.28	−2.74
3.77	247.9936	−0.0104	$C_6H_6N_3O_6S$	Vanillin sulphate	0.0216	MS/MS	3.27	
3.79	168.0406	0.0017	$C_8H_8O_4$	3,4-Dihydrophenylacetic acid	0.0402	MS/MS	2.54	
3.80	152.0458	0.0015	$C_8H_8O_3$	4-Hydroxyphenylacetic acid	0.0228	Database	−2.55	−3.41
3.81	163.0278	0.0025	$C_5H_9NO_3S$	*N*-Acetyl-L-cysteine	0.0216	MS/MS	2.85	
3.87	166.0664	−0.0034	$C_9H_{10}O_3$	Phenylacetic acid	0.0317	Database	−2.32	
4.00	339.0924	0.003	$C_{15}H_{17}NO_8$	5-Hydroxy-6-methoxyindole glucuronide	0.0216	MS/MS	3.83	3.85
4.02	383.1042	0.0035	$C_{14}H_{17}N_5O_8$	Succinyladenosine	0.0216	MS/MS	3.39	2.95
4.10	213.0063	0.0033	$C_8H_7NO_4S$	Indoxylsulphuric acid	0.0114	MS/MS		−2.20
4.13	152.0461	0.0012	$C_8H_8O_3$	*m*-Hydroxyphenylacetic acid	0.0402	MS/MS	2.28	
4.20	138.0286	0.0031	$C_7H_6O_3$	Salicylic acid	0.0256	MS/MS	2.86	
4.20	212.0654	0.0031	$C_{10}H_{12}O_5$	Vanillactic acid	0.0216	Database		2.4
4.34	133.0512	0.0016	C_8H_7NO	6-Hydroxyindole	0.0216	MS/MS	−2.92	2.95

4.45	159.0874	0.0021	$C_7H_{13}NO_3$	Acetyl-DL-valine	0.0228	MS/MS	3.4	
4.96	179.0336	0.0246	$C_9H_9NO_3$	Hippuric acid	0.0228	MS/MS	−2.89	−3.07
5.11	168.0411	0.0012	$C_8H_8O_4$	Vanillic acid	0.0216	MS/MS	−2.94	
5.23	146.0669	−0.0090	$C_6H_{10}O_4$	Monomethyl glutaric acid	0.0216	MS/MS	2.38	
5.24	124.0504	0.002	$C_7H_8O_2$	Salicyl alcohol	0.0216	MS/MS	−3.22	−3.44
5.36	218.1137	−0.0082	$C_{12}H_{14}N_2O_2$	Melatonin	0.0216	MS/MS	2.6	
5.57	122.0362	0.0006	$C_7H_6O_2$	Hydroxybenzaldehyde	0.0216	MS/MS	−3.35	
5.58	207.0858	0.0037	$C_{11}H_{13}NO_3$	*N*-Acetyl-L-phenylalanine	0.0216	MS/MS	−2.91	
5.79	209.0675	0.0013	$C_{10}H_{11}NO_4$	Hydroxyphenylacetylglycine	0.0228	Database	2.99	
5.83	188.0114	0.0029	$C_7H_8O_4S$	*p*-Cresol sulphate	0.0216	MS/MS	−2.86	−2.60
5.92	284.0464	0.0432	$C_{13}H_{16}O_7$	*p*-Cresol glucuronide	0.0216	MS/MS	3.31	2.92
6.13	166.0741	−0.0111	$C_9H_{10}O_3$	(±)-α-Methoxyphenylacetic acid	0.0216	MS/MS	−3.01	
6.79	203.1135	−0.0553	$C_{11}H_9NO_3$	3-(3-Indolyl)-2-oxopropanoic acid	0.0256	MS/MS		
6.86	246.0973	0.0031	$C_{13}H_{14}N_2O_3$	*N*-Acetyltryptophan	0.0256	MS/MS	2.78	
6.88	174.0732	0.016	$C_8H_{14}O_4$	Diethyl succinate	0.0216	MS/MS	−3.01	−2.26
7.06	218.0209	0.004	$C_8H_{10}O_5S$	Tyrosol-4-sulphate	0.0216	Database	−3.31	−2.68
8.40	336.1342	0.1322	$C_{21}H_{36}O_3$	Pregnanetriol	0.0256	Database	−2.53	
9.30	384.1518	0.0037	$C_{13}H_{25}O_7P$	DHAP(10:0)	0.0228	Database		−3.82
10.09	440.0588	−0.0002	$C_{10}H_{13}N_4O_{10}P$	Urate D-ribonucleotide	0.0216	Database		3.83
10.45	370.1841	−0.0027	$C_{19}H_{30}O_5S$	5α-Dihydrotestosterone sulphate	0.0114	MS/MS		3.1

Statistically significant (p <0.05) differences are shown for week 8 vs. pre-dose. q-values were adjusted for the false discovery rate (q <0.05). MS/MS indicates that the fragmentation of each identified metabolite was confirmed using the standard compound. ‘Database’ indicates that the fragmentation of each identified metabolite was searched in databases (HMDB and METLIN)

Table 8. Plasma metabolites identified by global metabolomic analysis in a positive ESI mode.

tR (min)	Mass (*m/z*)	Delta Da	Chemical formula	Identity	q-Value	Identification	UDCA vs pre-dose	Vit E vs pre-dose
6.01	180.0877	0.0022	$C_9H_{12}N_2O_2$	5-Hydroxykynurenamine	0.0006	MS/MS	−3.25	
5.82	265.1421	−0.0230	$C_{13}H_{16}N_2O_3$	6-Hydroxymelatonin	0.0094	Database	−2.94	
9.09	340.2337	0.0044	$C_{21}H_{34}O_2$	Epipregnanolone	0.0045	MS/MS	3.04	
11.29	381.2626	0.0018	$C_{18}H_{40}NO_5P$	Sphinganine phosphate	0.0101	MS/MS	2.93	
8.61	577.1917	0.4083	$C_{21}H_{34}N_3O_{10}SF_3$	4-Hydroxynonenal glutathione	0.0359	MS/MS	−2.70	
0.68	145.1108	0.0471	$C_7H_{19}N_3$	Spermidine	0.0011	MS/MS		3.03
0.67	117.0778	0.0012	$C_5H_{11}NO_2$	Betaine	0.0056	Database		2.80
0.69	271.1662	−0.0018	$C_{11}H_{21}N_5O_3$	Prolylarginine	0.0201	Database		−2.55
7.23	278.1638	−0.0008	$C_{15}H_{22}N_2O_3$	Phenylalanyl-isoleucine	0.0203	Database		−2.54
10.58	272.2127	0.0013	$C_{19}H_{28}O$	5a-Androst-3-en-17-one	0.0011	MS/MS		3.00
11.33	330.2434	−0.0028	$C_{18}H_{34}O_5$	(+)-9,10,18-Trihydroxy-12Z-octadecenoic acid	0.0398	Database		2.41
11.79	122.0727	0.0005	$C_8H_{10}O$	2,6-Dimethylphenol	0.007	Database		2.76
12.32	253.237	0.004	$C_{16}H_{31}NO$	Palmitoleamide	0.0398	MS/MS		2.41
12.46	297.2655	0.0015	$C_{18}H_{35}NO_2$	3-Ketosphingosine	0.017	Database		−2.59
13.96	299.2849	−0.0025	$C_{18}H_{37}NO_2$	Sphingosine	0.01	MS/MS		−2.70

Statistically significant ($p < 0.05$) differences are shown for week 8 vs. pre-dose. *q*-values were adjusted for the false discovery rate ($q < 0.05$). MS/MS indicates that the fragmentation of each identified metabolite was confirmed using the standard compound. ‘Database’ indicates that the fragmentation of each identified metabolite was searched in databases (HMDB and METLIN)

Metagenome profiling using urinary EVs

Global metabolomic profiling revealed that UDCA changed microbe-generated metabolites, such as phenylalanine, methoxyphenylacetic acid, hippuric acid, p-cresol, and N-acetyltryptophan. This suggested that the microbiota might be involved in bile acid regulation. To evaluate the relationship between microbial composition and responses to UDCA, metagenomic analysis was conducted using 16S ribosomal DNA (rDNA) sequencing before and after 8 weeks of each treatment. The composition of bacterial microbiota was investigated at the phylum and genus level by metagenomic analysis of bacteria-derived extracellular vesicles (EVs). Comparison of the alpha diversity in the UDCA and vitamin E treatment groups revealed no significant differences based on the Shannon index, as shown in Figure 18A and 18B. However, the Chao1 diversity index was lower at pre-dose than at week 8 in both UDCA and vitamin E treatment groups (Figure 19A and 19B). In Figure 18C and 18D, the beta diversity in the UDCA group shows clear separation at both phylum and genus levels. In the vitamin E group, however, the results appeared to be poorly clustered before and after 8 weeks of treatment at both levels (Figure 19C and 19D). The bar graphs of the 16S rDNA sequencing data indicate that UDCA and vitamin E significantly altered the microbial composition after 8 weeks of treatment (Figure 20). The relative abundance of *Bifidobacterium* markedly declined, by 77.5%, after UDCA treatment for 8 weeks, followed by *Lactobacillus* (64.8%) and *Lactobacillaceae* (85.7%), including all genera (Figure 21A-21C). These results are consistent with those of previous reports on the alteration of intestinal microbiota, including *Bifidobacterium* and

Lactobacillus, in obese individuals. Because the *Bacteroidetes*/*Firmicutes* ratio has been shown to be indicative of obesity in vivo, this ratio was also determined in this study (Figure 21E); however, there were no significant changes after UDCA treatment. Vitamin E treatment also changed the composition of certain bacteria. The greatest change in the relative abundance was shown for *Bacteroides*, in which case the relative abundance was reduced by 61.5% compared with that at pre-dose (Figure 21D). Similar to UDCA treatment, vitamin E treatment reduced the *Lactobacillaceae* abundance (Figure 21B). Interestingly, the ratio of *Bacteriodetes*/*Firmicutes* was lowered by vitamin E treatment (Figure 21E). Possible pathways involving bacterial modification are indicated in Figure 22.

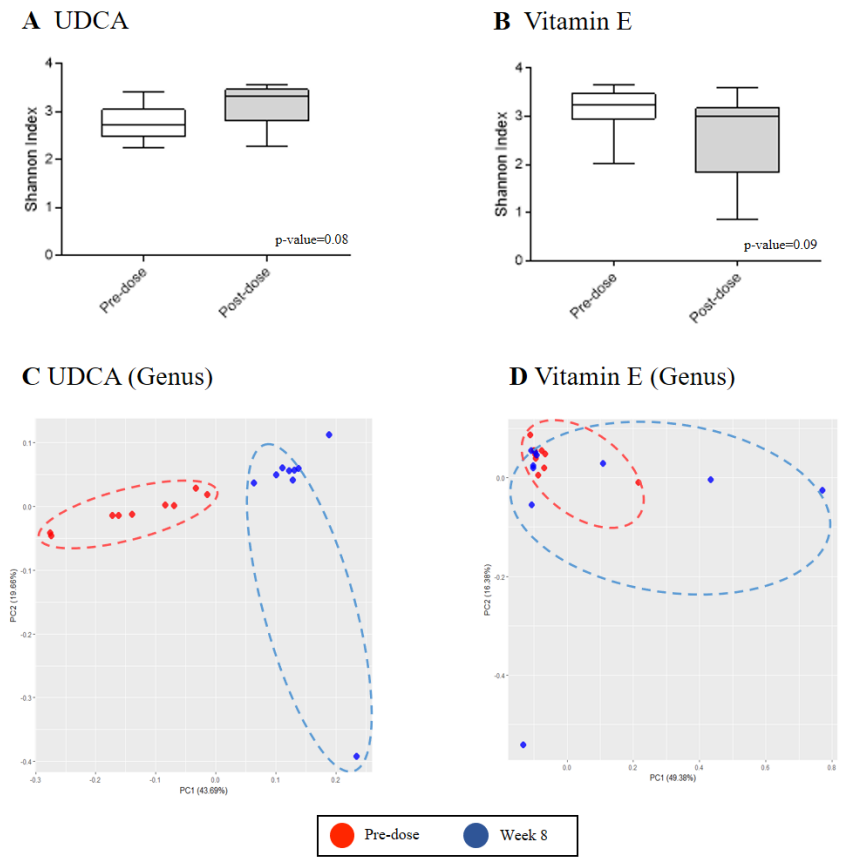

Figure 18. Alpha and beta diversity comparisons of microbiomes collected before and after UDCA treatment. Analyses were performed using sequencing data for the 16S rDNA V3 and V4 regions, with a rarefaction depth of 10,000 reads per sample. Whiskers in the boxplots represent the range of the minimum and maximum alpha diversity values within a population, excluding outliers. Alpha diversity was lower in EV samples collected before the treatment than in samples collected after the treatment. (A and B) Boxplots of the Shannon index for the UDCA and vitamin E groups, respectively. (C and D) Principal coordinate analysis of the UDCA and vitamin E treatment data at the genus level, respectively. The proportion of variance explained by each principal

coordinate axis is denoted in the corresponding axis label. Red and blue circles indicate samples at pre-dose and week 8, respectively

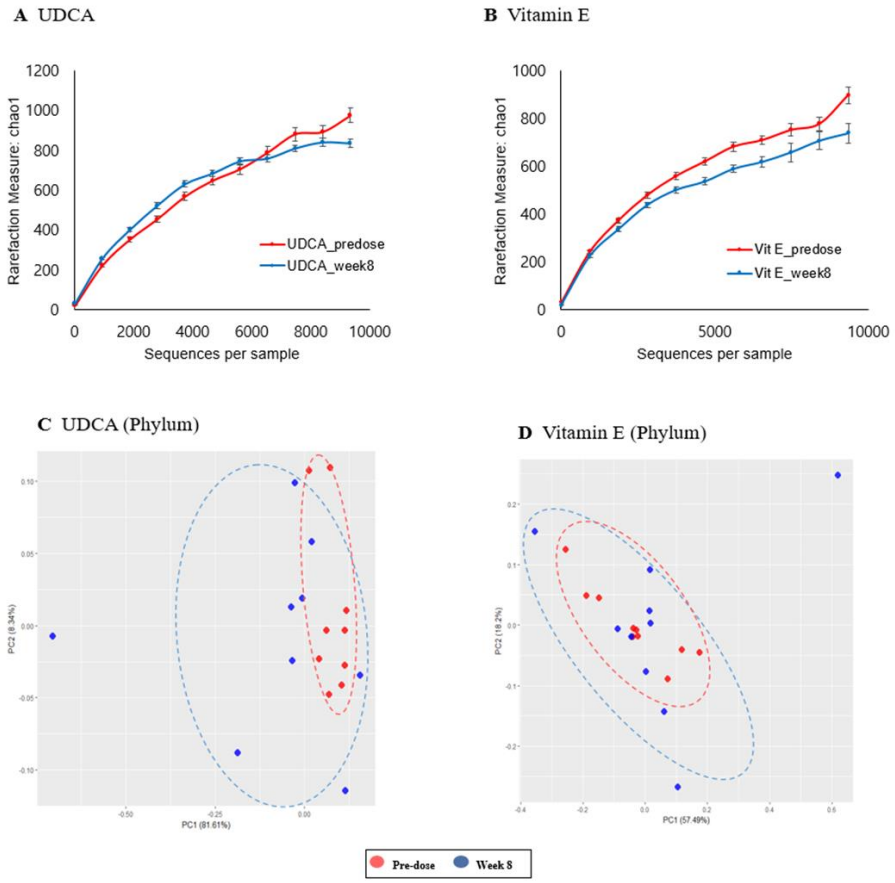

Figure 19. Chao1 score and beta diversity comparisons of microbiomes collected before and after UDCA and vitamin E treatments.

Analysis was performed using sequencing data for the 16S rDNA V3 and V4 regions, with a rarefaction depth of 10,000 reads per sample. Whiskers in the boxplot represent the range of the minimum and maximum alpha diversity values within a population, excluding outliers. Alpha diversity was lower in EV samples collected before the treatment than in those collected after the treatment. (A and B) Chao 1 scores of the UDCA and vitamin E groups, respectively. The results are expressed as the mean ± standard deviation. (C and D) Principal coordinate analysis (PCoA) of samples from the UDCA and

vitamin E treatment groups at the phylum level, respectively. The proportion of variance explained by each principal coordinate axis is denoted in the corresponding axis label. PCoA showed clear separation between samples collected before and after each treatment. Red and blue circles indicate samples collected at pre-dose and week 8, respectively

A Phylum

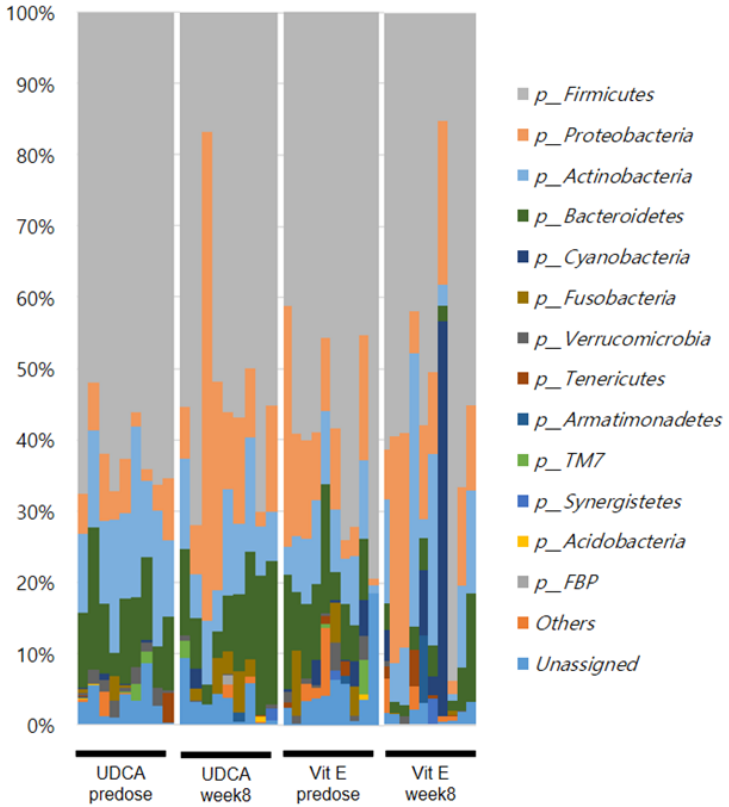

B Genus

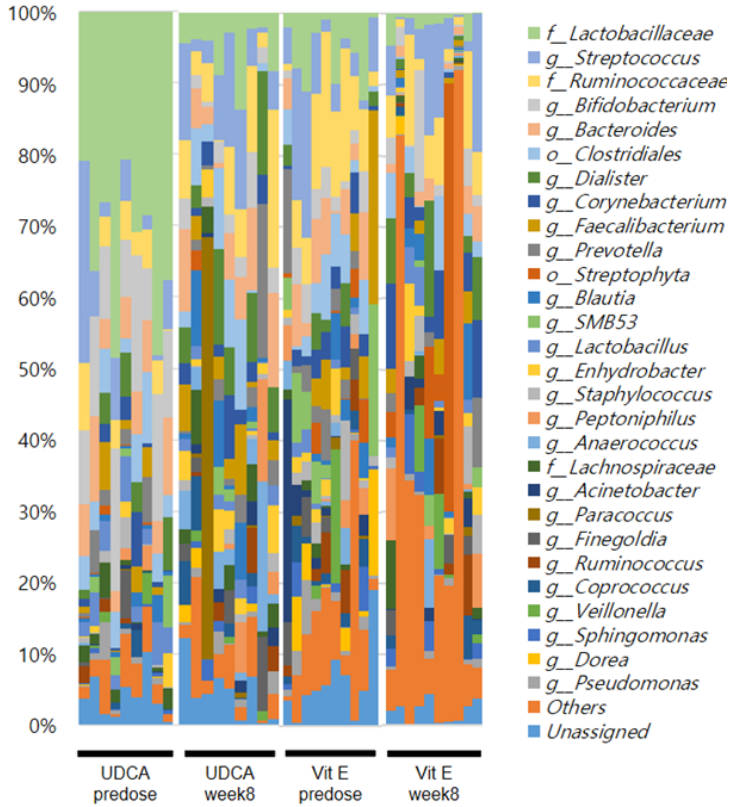

Figure 20. Taxonomic profiles of microbiomes collected before and after treatment. Analysis was performed using sequencing data for the 16S rDNA V3 and V4 regions, with a rarefaction depth of 10,000 reads per sample. (A) Plots of the relative taxon abundance for samples collected before and after UDCA or vitamin E treatment, summarised at the phylum level. Individual samples are presented along the horizontal axis, and relative taxon frequencies are denoted by the vertical axis. (B) Plots of the relative taxon abundance for samples collected before and after UDCA or vitamin E treatment, summarised at the genus level. Individual samples are presented along the horizontal axis, and relative taxon frequencies is denoted by the vertical axis

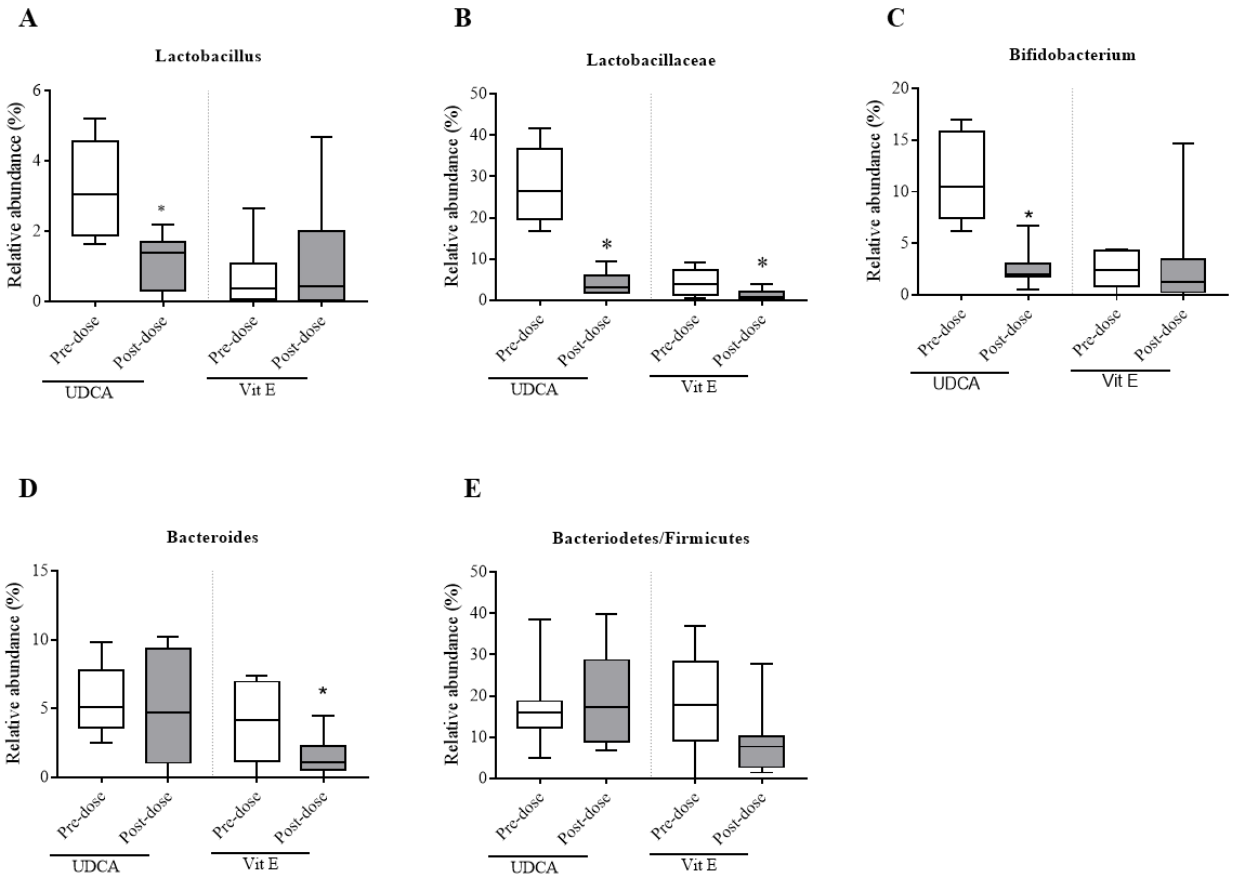
A
Lactobacillus
Relative abundance (%)
0
2
4
6
*
Pre-dose
Post-dose
Pre-dose
Post-dose
UDCA
Vit E
B
Lactobacillaceae
Relative abundance (%)
0
10
20
30
40
50
*
*
Pre-dose
Post-dose
Pre-dose
Post-dose
UDCA
Vit E
C
Bifidobacterium
Relative abundance (%)
0
5
10
15
20
*
Pre-dose
Post-dose
Pre-dose
Post-dose
UDCA
Vit E
D
Bacteroides
Relative abundance (%)
0
5
10
15
*
Pre-dose
Post-dose
Pre-dose
Post-dose
UDCA
Vit E
E
Bacteriodetes/Firmicutes
Relative abundance (%)
0
10
20
30
40
50
Pre-dose
Post-dose
Pre-dose
Post-dose
UDCA
Vit E

Figure 21. Changes in microbial compositions upon UDCA and vitamin E treatments. Relative bacterial abundances in the microbiome that distinctively changed after 8 weeks of UDCA or vitamin E treatment are shown in bar graphs. (A) *Lactobacillus*, (B) *Lactobacillaceae*, (C) *Bifidobacterium*, (D) *Bacteroides*, and (E) *Bacteroidetes*/*Firmicutes* ratio. The results are expressed as the mean ± standard deviation. * represents p-value <0.05 between pre-dose and week 8

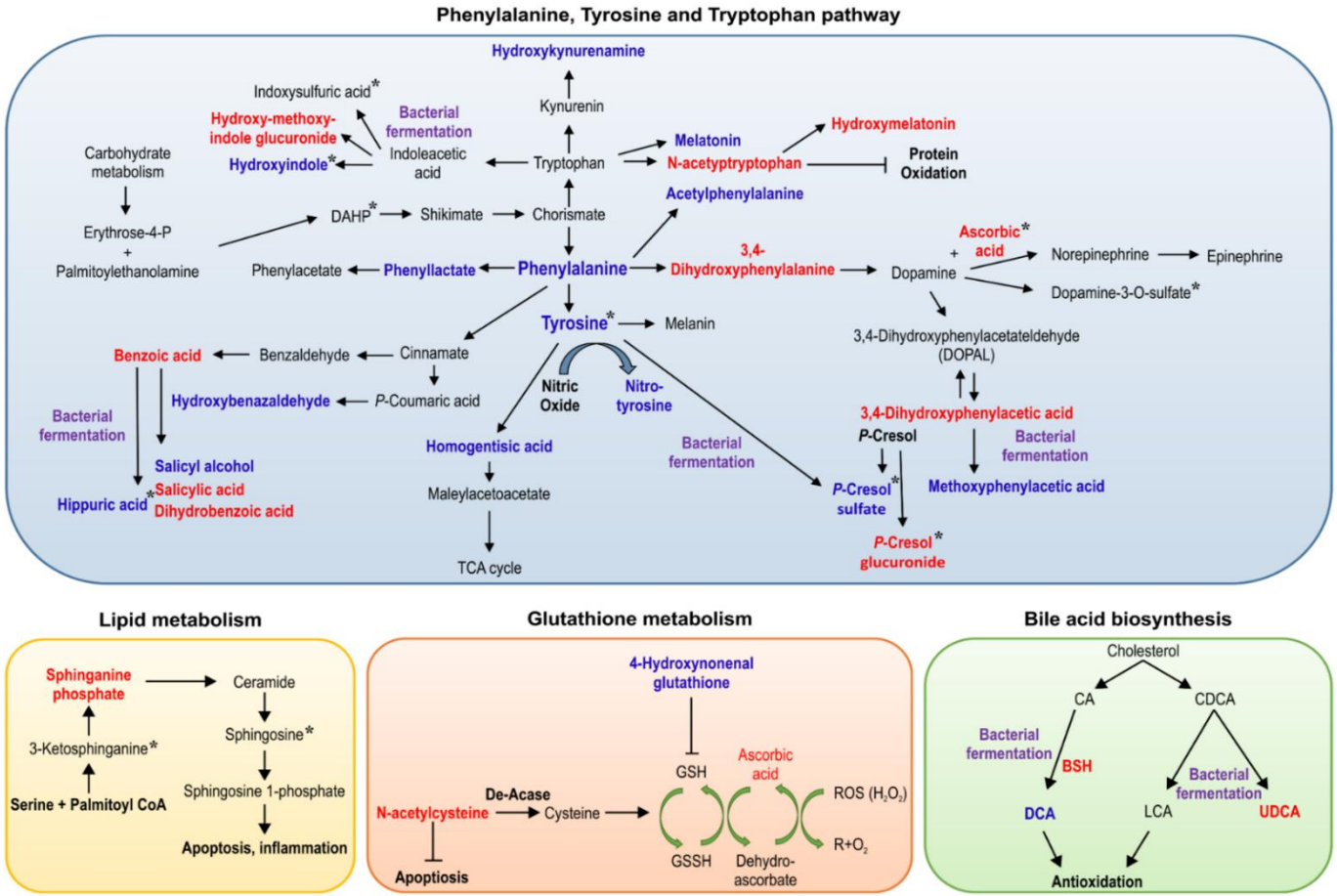
Phenylalanine, Tyrosine and Tryptophan pathway
Hydroxykynurenamine
Kynurenin
Indoxysulfuric acid*
Hydroxy-methoxy-indole glucuronide
Hydroxyindole*
Bacterial fermentation
Indoleacetic acid
Tryptophan
Melatonin
N-acetyptryptophan
Hydroxymelatonin
Protein Oxidation
Carbohydrate metabolism
Erythrose-4-P
+
Palmitoylethanolamine
DAHP*
Shikimate
Chorismate
Acetylphenylalanine
Phenylacetate
Phenyllactate
Phenylalanine
3,4-Dihydroxyphenylalanine
Ascorbic* acid
Dopamine
Norepinephrine
Epinephrine
Dopamine-3-O-sulfate*
Tyrosine*
Melanin
3,4-Dihydroxyphenylacetateldehyde (DOPAL)
Benzoic acid
Benzaldehyde
Cinnamate
Nitric Oxide
Nitro-tyrosine
Hydroxybenazaldehyde
P-Coumaric acid
3,4-Dihydroxyphenylacetic acid
P-Cresol
Bacterial fermentation
Methoxyphenylacetic acid
Bacterial fermentation
Salicyl alcohol
Salicylic acid
Dihydrobenzoic acid
Hippuric acid*
Homogentisic acid
Maleylacetoacetate
TCA cycle
P-Cresol sulfate*
P-Cresol glucuronide*
Lipid metabolism
Sphinganine phosphate
Ceramide
Sphingosine*
Sphingosine 1-phosphate
3-Ketosphinganine*
Serine + Palmitoyl CoA
Apoptosis, inflammation
Glutathione metabolism
4-Hydroxynonenal glutathione
GSH
Ascorbic acid
ROS (H_2O_2)
De-Acase
N-acetylcysteine
Cysteine
$R+O_2$
GSSH
Dehydro-ascorbate
Apoptiosis
Bile acid biosynthesis
Cholesterol
CA
CDCA
Bacterial fermentation
BSH
Bacterial fermentation
DCA
LCA
UDCA
Antioxidation

Figure 22. Schematic diagram of potential therapeutic mechanisms of UDCA treatment. Metabolomic analysis revealed that UDCA reduces major compounds in the phenylalanine/tyrosine and tryptophan pathways, including phenylalanine, phenyllactate, acetylphenylalanine, 3,4-hydroxyphenylacetate aldehyde, dopamine-3-O-sulphate, hydroxybenzaldehyde, p-cresol sulphate, melatonin, hydroxykynurenamine, hydroxyindole, and hippuric acid, in the plasma and urine. Intermediate metabolites such as hydroxymelatonin, benzoic acid, and salicylic acid, were induced. Strong antioxidants such as ascorbate, acetyltryptophan, and N-acetyl-L-cysteine were elevated. Further, detoxification of uremic toxins by glucuronidation (hydroxymethoxyindole glucuronide and p-cresol glucuronide) was observed after UDCA treatment. However, vitamin E reduced indole propionic acid, indoxyl sulphate, 3-ketosphinganine, and sphingosine, which were not regulated by UDCA. Blue colour indicates a decrease in the metabolite level, and red colour indicates an increase in the metabolite level after UDCA treatment. Metabolites that changed after vitamin E treatment are marked with an asterisk (*). Metabolites that were possibly regulated by bacterial modification are marked with a purple colour

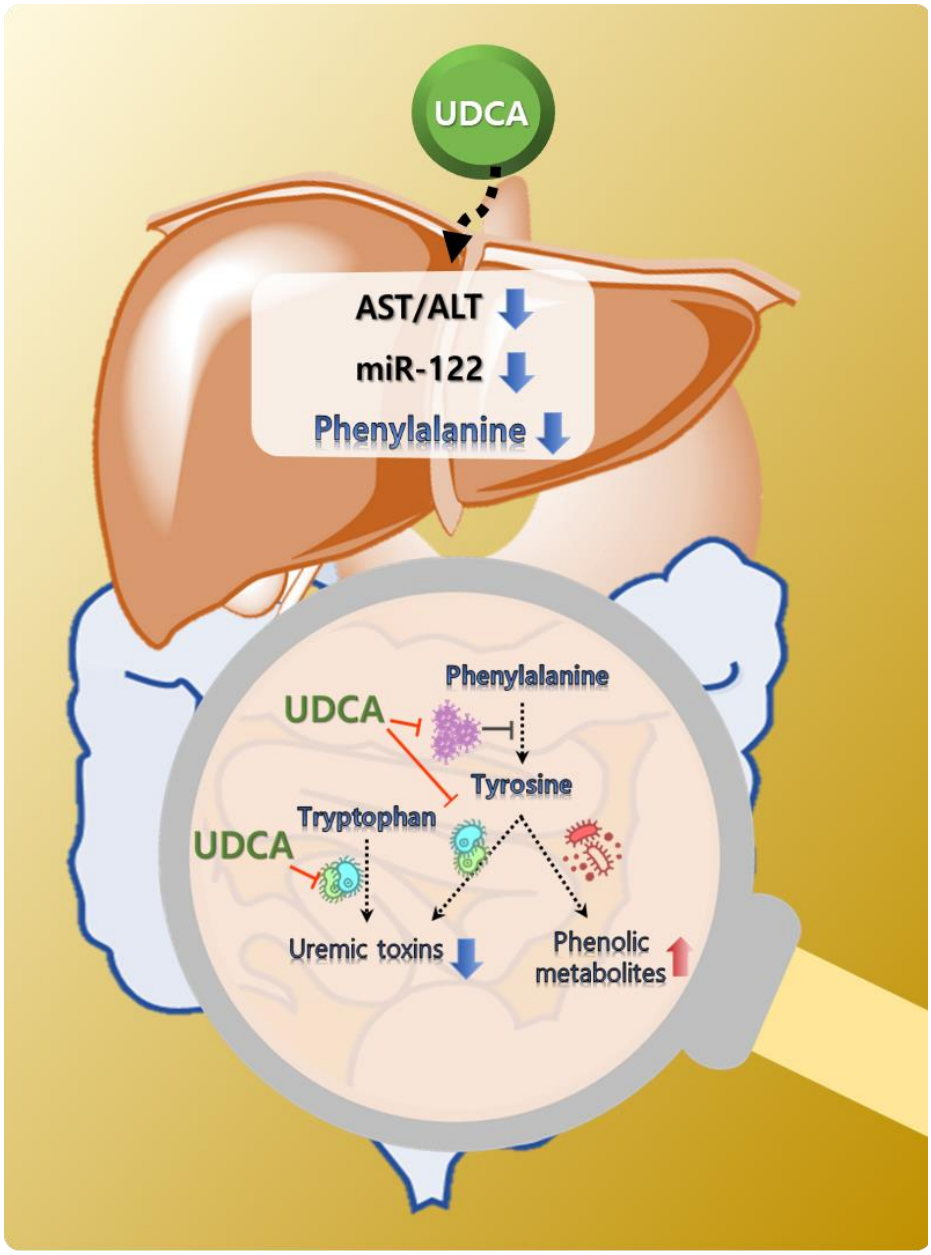

Figure 23. Schematic diagram summarizing therapeutic effects of UDCA treatment in healthy and liver dysfunction subjects. UDCA was effective to reduce circulating AST, ALT and miR-122 in both healthy and liver dysfunction subjects. Metabolomics profiling revealed that UDCA predominantly regulated the level of phenylalanine and its metabolites in both

studies. Also, urinary metabolomics profiling resulted the increase of flavonoids in healthy subjects and, the regulation of uremic toxins and antioxidants which are downstream of aromatic amino acids; phenylalanine, tyrosine and tryptophan was observed in liver dysfunction subjects. The correlation of metabolites and UDCA was further evaluated by analysing metagenome profiling of bacteria-derived extracellular vesicles and therefore, it was assumed that gut-microbiome may contribute on the metabolic changes of UDCA. Decreased level of metabolites and serum parameters were indicated by blue-coloured arrow and increased level of metabolites were indicated by red-coloured arrow

DISCUSSION

PART I & PART II. Hepatoprotective effects of UDCA in healthy subjects

In this study, global metabolomic approach was used to assess hepatoprotection in healthy young and elderly subjects. Young subjects were treated with high (1200 mg), intermediate (800 mg), or low (400 mg) doses of UDCA and elderly subjects were treated with intermediate (800 mg) or low (400 mg) dose of UDCA for 2 weeks, thereby reducing levels of the liver dysfunction biomarkers ALT, AST, and miR-122, even at low doses. UDCA also increased plasma level of UDCA, GUDCA and TUDCA and significantly reduced hydrophobic bile acid, TDCA after 2 weeks. Through global metabolomics analyses using LC/QTOFMS and GC/TOFMS, metabolic signatures including amino acid, flavonoid, and fatty acid metabolism were revealed in young subjects. Unfortunately, there was no notable observation in global metabolomics analysis of elderly subjects.

UDCA has long been used to treat PBC and non-alcoholic steatohepatitis (NASH), as it decreases liver biochemical levels, including alkaline phosphatase and gamma-glutamyltransferase (GGT), and delays the need for liver transplantation [19, 20]. Numerous studies have attempted to investigate the mechanisms underlying the beneficial effects of UDCA in liver dysfunction. Experimental evidence suggests three major mechanisms of action of UDCA: cholangiocyte protection against cytotoxicity of hydrophobic bile acids, stimulation of hepatobiliary secretion, and hepatocyte protection against bile

acid-induced apoptosis. One or all of these mechanisms may be occur in individual cholestatic disorders and/or different stages of cholestatic liver disease [21].

In the present study, UDCA treatment effectively reduced the ALT/AST score even upon short-term administration, which was anticipated to a certain degree based on previous studies [1, 3, 14, 15]. However, the scores were below the upper limits of normal ALT and AST values since this clinical trial was conducted in healthy men. However, miR-122 levels did not encounter this limitation. miR-122 is the most prevalent miRNA in the adult liver, accounting for approximately 70% of the total liver miRNA population [18]. It regulates liver-enriched transcription factors, including hepatocyte nuclear factor-4 α and p53 [22, 23], thereby maintaining an appropriate balance between hepatocyte proliferation and differentiation. miR-122 is reportedly up-regulated in patients with hepatitis C and NAFLD [18]. In the previous study, miR-122 was also used as an early biomarker of drug-induced liver injury [24]. UDCA significantly decreased miR-122 levels, thereby conclusively indicating its hepatoprotective effect. However, it is interesting here that even short-term administration of a low UDCA dosage was sufficient to modulate miR-122 expression levels and liver function scores. This may indicate that lower doses of UDCA may be more effective for ameliorating or preventing liver dysfunction at pre-PBC stages with no adverse effects.

Global metabolomics analysis using LC/QTOFMS and GC/TOFMS enabled the evaluation of the mechanisms of action of UDCA. Among the new findings obtained herein, most of the identified metabolites categorized as amino acids

were decreased upon UDCA treatment. In particular, urine and plasma levels of phenylalanine metabolites, including alanine and phenylalanine, were strongly regulated by UDCA. Amino acids are metabolized to provide energy or used to synthesize other bioactive molecules. In particular, aromatic amino acids are primarily metabolized in the liver [25, 26]. Increased plasma levels of these metabolites suggest an increase in the degradation of muscle proteins and decreased metabolism of these amino acids in the liver [26]. This implies that high concentrations of amino acids result in hepatotoxicity. Systemic phenylalanine and aminotransaminase levels are positively correlated with age [27]. A recent *in vivo* study reported that FXR activation via the administration of obeticholic acid as part of high-protein diets enhanced hepatic amino acid catabolism via the regulation of amino acid-degrading enzymes [28]. Nevertheless, blunted FXR activity downregulated these enzymes and appeared to reduce phenylalanine, alanine, and glutamine levels. As reported previously, it is possible that the regulation of amino acids might be influenced by FXR activation. However, to ascertain whether FXR directly regulates amino acid catabolism or biosynthesis, further studies involving liver and/or intestinal-specific FXR deletion models are required.

Another possible contributor to amino acid levels is the transport of bile acid through the solute carrier (SLC) family of transport proteins during enterohepatic recirculation. The SLC gene superfamily encodes membrane-bound transporters which play a crucial role in passive transport, symport, and antiport with substrates including amino acids, inorganic cations, and anions. Solute carrier family 10 (SLC10) comprises two sodium-dependent bile acid

transporters: the Na^+/taurocholate cotransporting polypeptide (NTCP; SLC10A1) and the apical sodium-dependent bile acid transporter (ASBT; SLC10A2), located in the liver and small intestine, respectively [29, 30]. SLC36 enables the transport of proton-coupled amino acids and SLC43 represents the sodium-independent system-L-like amino acid [31]. The most common feature shared by these transporters is that they rely on a sodium gradient to actively penetrate cells [30]. Therefore, sodium gradient-dependent bile flow may counteract the reabsorption of amino acids into the systemic circulation.

Elevated levels of phosphatidylcholine (PC), lyso-PC, phosphoethanolamine (PE), and sphingomyelins (SM) were previously reported as biomarkers of liver diseases including non-alcoholic fatty liver disease (NAFLD) [32-35]. In particular, PC accounts for ~95% of choline-containing compounds and is secreted into the plasma along with lipoproteins. These phospholipid classes are associated with inflammation and cellular apoptosis [34, 35]. In the present study, plasma PC, lyso-PC, and PE levels decreased significantly after treatment with UDCA. This may be clinically acceptable because its therapeutic implications have been reported in patients with mutations in canalicular transporters including ATP8B1, ABCB11, and ABCB4 [36]. Canalicular transporters are the major route for phospholipids and UDCA has been proven to propagate their flux, thereby decreasing systemic phospholipid levels [36]. Furthermore, the elevation of linoleic acid (a long-chain ω-6 polyunsaturated fatty acid) may be associated with the regulation of these fatty acids and some cytokines by targeting sterol regulatory element-binding protein (SREBP)-1

isomers [37-39].

Ferulic acid-, fertaric acid-, caffeic acid-, and vanillin-containing metabolites are hydroxycinnamic acids and are classified as a type of polyphenol. These phenolic compounds are ubiquitous in vegetables and fruits, thereby only being capable of being consumed as/with food. The free forms of these phenolic acids are primarily distributed in the liver and conjugated primarily with glucuronide/sulfate and secreted into the bile for enterohepatic circulation [40-42]. Certain free compounds and their conjugates in the systemic circulation and tissues are then metabolized into other compounds, whereas most of them are ultimately eliminated through the kidneys [40, 41, 43]. Although the mechanisms underlying phenol metabolism are yet unclear, some studies have reported that dietary phenolic acids required bacterial enzymatic activity to be transformed or degraded. For example, *Lactobacillus mucosae*, *Enterococcus faecium*, and *Bifidobacterium lactis* possess enzymes for the esterification of hydroxycinnamates and isoflavones [44, 45]. Dehydroxylation of these compounds is associated with *Clostridium scindens* and *Eggerthella lenta* [46, 47]. After transformation, the compounds passively permeate through the intestinal epithelium via transcellular diffusion into the blood or other tissues [40, 41, 43, 48, 49]. Based on previous reports, it was assumed that two possible mechanisms explaining the high levels of phenolic compounds observed in this study. First, dietary phenols in bile might be reabsorbed in the same manner as UDCA - predominantly transported via passive diffusion in the small intestine. Alternatively, changes in the gut microbiota upon UDCA treatment may have influenced further metabolic reactions involving dietary phenols, thereby

rendering them available for reabsorption or excretion via bile. Further investigations are, however, required to completely elucidate the interaction of dietary phenols and gut microbiota. Particularly, future studies should investigate whether microbiomes regulated by UDCA display enzymatic activity on dietary phenols for transformation.

Diminished phenylalanine levels were present in UDCA-treated individuals regardless of whether they had pre-existing conditions or were healthy. In addition, UDCA enabled the regulation of uremic toxins such as p-cresol sulfate and hippuric acid in patients. However, UDCA exerted anti-oxidative effects in healthy subjects. Therefore, it is suggested with caution that short term treatment with a non-toxic dose of UDCA may prevent liver dysfunction at a very early stage, presenting a possible new therapeutic strategy for healthy individuals or those with mild liver dysfunction.

Mechanistic studies on such therapeutic interventions in healthy subjects might be interpreted inconsistently relative to those involving patents with disease. However, this study reported changes in a putative early biomarker of liver injury (miR-122) upon UDCA treatment, therefore enabling the further evaluation of pharmacological mechanisms. However, small sample size likely compromised the statistical power of the results, thereby serving as a study limitation. Future studies evaluating the interaction between gut microbiota and dietary phenolic acids are required to potentiate the therapeutic effects of UDCA administration on human health.

In elderly subjects, effective regulation on liver function was not observed by UDCA. Low dosage of UDCA (1200 mg treatment was absent in elderly

subject) might be the cause of less effectiveness. Otherwise, aging-related changes in hepatocytes may influence on the efficacy of UDCA. With aging, the volume of blood flow of the liver gradually decrease by 20-40% as one gets older. Enhanced portion of lipofuscins in hepatocytes also cause increased generation of oxidative stress such as reactive oxygen species [50-52]. Due to those factors regarding aging process, elderly subjects might be required higher dosage of UDCA to show significant therapeutic effects.

Together, this study demonstrated changes in metabolite levels following UDCA treatment in healthy men, and the data indicates that a potentially novel therapeutic strategy using UDCA may be possible.

PART III. Hepatoprotective effects of UDCA in patients with liver dysfunction

In this study, it was found that UDCA regulated metabolic pathways (mainly the phenylalanine/tyrosine pathway), reduced the miR-122 expression level, remodelled the microbiome, and changed the bile acid content, thus exerting protective effects on liver function. A potent antioxidant, vitamin E, also lowered the levels of liver function parameters such as AST, ALT, and GGT in the serum but did not distinctly regulate bile acids.

UDCA has long been used for the treatment of PBC and non-alcoholic steatohepatitis (NASH) because it decreases liver biochemical parameters, including alkaline phosphatase and GGT, and delays the need for liver transplantation [19, 20]. However, the benefits of UDCA for liver disease have

remained controversial. Thus, Ratziu et al. have reported that even at high doses of UDCA (25–35 mg/kg/day), administered for 12 months, no therapeutic effects were observed in patients with NASH [15]. On the other hand, Dufour et al. have reported a positive effect after UDCA treatment for 2 years [14].

In this study, UDCA treatment effectively reduced liver enzymes (AST, ALT, and GGT). However, the AST and ALT levels were not significantly reduced in the UDCA group at week 8 because one subject appeared to have had dramatic increases in serum parameters, including cholesterol levels, and showed contrasting results in metabolomic profiling (data not shown). UDCA also significantly reduced the circulating miR-122 level, which has been used as an early diagnostic biomarker of liver damage [23]. As shown in Table 6, the miR-122 level started to decrease at week 4 of UDCA administration. Vitamin E treatment also decreased the miR-122 level at week 4, but the decrease was not significant. UDCA is known to regulate the levels of hydrophobic bile acids, such as LCA and DCA conjugates, by increasing the total bile acid pool size, thereby lowering the cytotoxicity [19]. To measure bile acids at the level of enterohepatic circulation, targeted metabolomic analysis was performed (Figure 15). As expected, UDCA and its conjugates, TUDCA and GUDCA, gradually increased, whereas the DCA level decreased after 8 weeks of treatment. Meanwhile, vitamin E did not cause any typical alterations in the levels of bile acids. These data reveal that UDCA controls hydrophobic bile acids and miR-122 in liver dysfunction patients.

Global metabolomics has recently been used to identify a panel of metabolic biomarkers that help distinguish between the stages of liver disease,

including NAFLD, NASH, and cirrhosis [33, 53, 54]. Despite numerous studies supporting the efficacy of UDCA in NASH, metabolomic profiling has not been previously conducted to elucidate its protective mechanisms.

Using metabolomic analysis, the capacity of UDCA as an antioxidant was examined. The elevated levels of uremic toxins (hippuric acid and *p*-cresol) and oxidative stress markers (3-nitrotyrosine and 4-HNE GSH) were controlled in the NAFLD patients after 8 weeks of treatment with UDCA. 3-Nitrotyrosine is a cytotoxic molecule, reducing the cell survival, and 4-HNE GSH is a product of 4-HNE conjugation with GSH, resulting from lipid peroxidation [55]. UDCA increased the *N*-acetylcysteine content, resulting in increased synthesis of GSH and ascorbic acid. UDCA has been reported to activate nuclear factor (erythroid-derived 2)-like 2 (NRF2) signalling in PBC patients [6]. As shown in Figure 17, Table 7 and Table 8, some metabolites of the phenylalanine pathway (4-hydroxybenzenesulphonic acid, 4-hydroxyphenylacetic acid, and salicyl alcohol), uremic toxins (hippuric acid and *p*-cresol sulphate), and antioxidants (*N*-acetylcysteine and ascorbic acid) were identified as metabolomic candidates in the UDCA group. In addition, vitamin E reduced tryptophan-originated uremic toxins and lowered some inflammatory lipids. Most regulatory mechanisms of UDCA are related to phenylalanine/tyrosine metabolism, while those of vitamin E are directly related to inflammatory metabolites. The data of metabolomic profiling suggested different regulatory mechanisms for UDCA and vitamin E against liver damage.

Apart from bile acid regulation, imbalanced production of AAAs and BAAs as circulating biomarkers of liver damage has frequently been reported

[33, 54]. In particular, an increased ratio of AAAs to BAAs has been suggested as a circulating biomarker of NAFLD [54]. Interestingly, several abundant metabolites, distinctively changed in the UDCA group, were associated with the phenylalanine/tyrosine pathway. Most of them were reduced after 8 weeks of treatment. A positive correlation between phenylalanine and ALT has been suggested; however, there is still no adequate evidence [27]. The liver is the predominant site of phenylalanine metabolism; therefore, deterioration of liver function, indicated by abnormally high levels of aminotransaminases (ALT, AST, and GGT), may decrease phenylalanine metabolism, thereby increasing its systemic level.

Changes in AAAs may be associated with the gut microbiome. *N*-acetyltryptophan, 6-hydroxyindole, and 5-hydroxy-6-methoxyindole glucuronide are tryptophan intermediates, well known to be bacteria-derived metabolites. Treatment modalities depend on circulating levels of tryptophan, phenylalanine, and tyrosine [56]. Therefore, the fluctuations in microbial composition was examined during drug treatment. It is well known that gut bacteria secrete small molecules to communicate with the host; bacteria-produced EVs contain various molecules, including proteins, nucleic acids, and lipids, and easily travel within the host body, independent of transporters. EVs are ubiquitously produced by all gram-negative and some gram-positive bacteria, and their presence in biofluids can be used to assess microbial compositions [57-59]. Recently, an EV-based metagenomics study has been used to determine diagnostic biomarkers for pregnancy [58], atopic dermatitis [57], and type 2 diabetes [60].

It was found that UDCA reduced the levels of *Lactobacillus* and *Bifidobacterium* after 8 weeks of treatment. *Lactobacillus-, Bifidobacterium-, Bacteroides-,* and *Clostridium*-rich microbiomes have been found to interrupt the synthesis of gut bacterial metabolites [61]. UDCA reduced the levels of phenylalanine/tyrosine and tryptophan metabolites as shown in Figure 17, Table 7 and Table 8. However, it remains unclear whether the microbiota directly control the synthesis of these aromatic amino acids or inhibit their metabolism. Vitamin E treatment reduced the abundance of *Bacteroidetes* and decreased the ratio of *Bacteroidetes/Firmicutes* at week 8 (Figure 21E). Although the relationship between vitamin E and *Bacteroidetes* has not been demonstrated yet, a recent study has reported that vitamin E supplementation effectively lowers the inflammatory response and *Bacteroidetes* abundance in infants with iron deficiency [62].

A study combining metabolomics and metagenomic analysis has suggested that administration of Tempol (4-hydroxy-2,2,6,6-tetramethylpiperidin-1-oxyl) inhibits farnesoid X receptor (FXR) signalling, resulting in bile acid dysregulation, and reduces the *Lactobacillus* abundance and bile salt hydrolase (BSH) activity in obese animals [16]. BSH, produced by *Lactobacillus* and *Bifidobacterium*, catalyses the deconjugation of glycine or taurine derivatives of bile acids, especially DCA and LCA [63]. The mechanism of BSH in bile regulation is a matter of controversy. Theoretically, BSH dehydrolases bile acids, leading to their recycling through enterohepatic circulation, which is beneficial to the host; however, unconjugated forms are more hydrophobic and require active excretion [63]. Although the results are in

partial agreement with those of previous reports, this study presents some limitations. First of all, placebo-controlled examination is omitted in this study. Although vitamin E has been well known as a potent antioxidant, liver dysfunction is not the indication of the treatment therefore, it may not be appropriate to use vitamin E as a positive control group. Also, further evaluation of study is required to compare the changes in microbial composition at the faecal level to confirm the results of EVs. Taken together, it was suggested that intestinal host–microbiome interactions play diverse roles in the pathophysiological process and may exert therapeutic effects.

CONCLUSION

In the study with healthy young subject, this study uses a metabolomics approach involving LC/QTOFMS and GC/TOFMS to evaluate potential therapeutic mechanisms of UDCA in healthy men. The findings suggest that UDCA effectively improved liver function and decreased circulating miR-122 levels. The possible mechanisms underlying this hepatoprotection may involve metabolic modifications in amino acid, flavonoid, and fatty acid metabolism.

UDCA treatment on elderly subjects were also seemed to be effective to regulate ALT score but there was apparent regulation of liver function scores, bile acid profiling and global metabolomics analyses.

The study on patients with liver dysfunction was the first study to apply a systematic approach, using targeted and global metabolomics and metagenomic analysis, to elucidate the underlying mechanisms of UDCA effects in patients with liver dysfunction. The findings suggest that UDCA effectively improves the liver function through various mechanisms, including bile acid regulation, metabolism regulation, and relevant microbiome remodelling, as well as by exerting antioxidant effects similar to those of vitamin E.

The schematic diagram summarizing the effects of UDCA was shown in Figure 23.

REFERENCES

1. Beuers, U., et al., *New paradigms in the treatment of hepatic cholestasis: from UDCA to FXR, PXR and beyond.* J Hepatol, 2015. **62**(1 Suppl): p. S25-37.
2. Fiorucci, S., M. Biagioli, and E. Distrutti, *Future trends in the treatment of non-alcoholic steatohepatitis.* Pharmacol Res, 2018. **134**: p. 289-298.
3. Parikh, P., et al., *An open-label randomized control study to compare the efficacy of vitamin e versus ursodeoxycholic acid in nondiabetic and noncirrhotic Indian NAFLD patients.* Saudi J Gastroenterol, 2016. **22**(3): p. 192-7.
4. Roma, M.G., et al., *Ursodeoxycholic acid in cholestasis: linking action mechanisms to therapeutic applications.* Clin Sci (Lond), 2011. **121**(12): p. 523-44.
5. Sanchez-Garcia, A., et al., *Effect of ursodeoxycholic acid on glycemic markers: A systematic review and meta-analysis of clinical trials.* Pharmacol Res, 2018. **135**: p. 144-149.
6. Kawata, K., et al., *Enhanced hepatic Nrf2 activation after ursodeoxycholic acid treatment in patients with primary biliary cirrhosis.* Antioxid Redox Signal, 2010. **13**(3): p. 259-68.
7. Mueller, M., et al., *Ursodeoxycholic acid exerts farnesoid X receptor-antagonistic effects on bile acid and lipid metabolism in morbid obesity.* J Hepatol, 2015. **62**(6): p. 1398-404.
8. Gonzalez, F.J., et al., *Inhibition of farnesoid X receptor signaling shows beneficial effects in human obesity.* Journal of Hepatology, 2015. **62**(6): p. 1234-1236.
9. Trauner, M. and I.W. Graziadei, *Review article: mechanisms of action and therapeutic applications of ursodeoxycholic acid in chronic liver diseases.* Aliment Pharmacol Ther, 1999. **13**(8): p. 979-96.
10. Johnson, C.H., J. Ivanisevic, and G. Siuzdak, *Metabolomics: beyond biomarkers and towards mechanisms.* Nat Rev Mol Cell Biol, 2016. **17**(7): p. 451-9.
11. Pan, X., et al., *Metabolomic Profiling of Bile Acids in Clinical and Experimental Samples of Alzheimer's Disease.* Metabolites, 2017. **7**(2).
12. Jahnel, J., et al., *Inflammatory bowel disease alters intestinal bile acid transporter expression.* Drug Metab Dispos, 2014. **42**(9): p. 1423-31.
13. Wunsch, E., et al., *Prospective evaluation of ursodeoxycholic acid withdrawal in patients with primary sclerosing cholangitis.* Hepatology, 2014. **60**(3): p. 931-40.
14. Dufour, J.F., et al., *Randomized placebo-controlled trial of ursodeoxycholic acid with vitamin e in nonalcoholic*

steatohepatitis. Clin Gastroenterol Hepatol, 2006. **4**(12): p. 1537-43.
15. Leuschner, U.F., et al., *High-dose ursodeoxycholic acid therapy for nonalcoholic steatohepatitis: a double-blind, randomized, placebo-controlled trial.* Hepatology, 2010. **52**(2): p. 472-9.
16. Li, F., et al., *Microbiome remodelling leads to inhibition of intestinal farnesoid X receptor signalling and decreased obesity.* Nat Commun, 2013. **4**: p. 2384.
17. Chakraborti, C.K., *New-found link between microbiota and obesity.* World J Gastrointest Pathophysiol, 2015. **6**(4): p. 110-9.
18. Bandiera, S., et al., *miR-122--a key factor and therapeutic target in liver disease.* J Hepatol, 2015. **62**(2): p. 448-57.
19. Haedrich, M. and J.F. Dufour, *UDCA for NASH: end of the story?* J Hepatol, 2011. **54**(5): p. 856-8.
20. Nevens, F., et al., *A Placebo-Controlled Trial of Obeticholic Acid in Primary Biliary Cholangitis.* N Engl J Med, 2016. **375**(7): p. 631-43.
21. Paumgartner, G. and U. Beuers, *Ursodeoxycholic acid in cholestatic liver disease: Mechanisms of action and therapeutic use revisited.* Hepatology, 2002. **36**(3): p. 525-531.
22. Mukherjee, S., et al., *Role of plasma amino acids and gaba in alcoholic and non-alcoholic fatty liver disease-a pilot study.* Indian J Clin Biochem, 2010. **25**(1): p. 37-42.
23. Vincent, R. and A. Sanyal, *Recent Advances in Understanding of NASH: MicroRNAs as Both Biochemical Markers and Players.* Curr Pathobiol Rep, 2014. **2**(3): p. 109-115.
24. Lee, J., et al., *Exploration of Biomarkers for Amoxicillin/Clavulanate-Induced Liver Injury: Multi-Omics Approaches.* Clin Transl Sci, 2017. **10**(3): p. 163-171.
25. Rui, L., *Energy metabolism in the liver.* Compr Physiol, 2014. **4**(1): p. 177-97.
26. Kamata, S., et al., *Early postoperative change of plasma levels of amino acids in neonates with perforative peritonitis and its prognostic significance.* J Pediatr Surg, 1995. **30**(4): p. 559-62.
27. Jung, S., et al., *Age-related increase in alanine aminotransferase correlates with elevated levels of plasma amino acids, decanoylcarnitine, Lp-PLA2 Activity, oxidative stress, and arterial stiffness.* J Proteome Res, 2014. **13**(7): p. 3467-75.
28. Massafra, V., et al., *Farnesoid X Receptor Activation Promotes Hepatic Amino Acid Catabolism and Ammonium Clearance in Mice.* Gastroenterology, 2017. **152**(6): p. 1462-1476 e10.
29. Balakrishnan, A. and J.E. Polli, *Apical sodium dependent bile acid transporter (ASBT, SLC10A2): a potential prodrug target.* Mol Pharm, 2006. **3**(3): p. 223-30.
30. Geyer, J., T. Wilke, and E. Petzinger, *The solute carrier family SLC10: more than a family of bile acid transporters regarding*

function and phylogenetic relationships. Naunyn-Schmiedebergs Archives of Pharmacology, 2006. **372**(6): p. 413-431.
31. He, L., K. Vasiliou, and D.W. Nebert, *Analysis and update of the human solute carrier (SLC) gene superfamily.* Hum Genomics, 2009. **3**(2): p. 195-206.
32. Ma, D.W., et al., *Plasma phospholipids and fatty acid composition differ between liver biopsy-proven nonalcoholic fatty liver disease and healthy subjects.* Nutr Diabetes, 2016. **6**(7): p. e220.
33. Chang, H., et al., *Identification of key metabolic changes during liver fibrosis progression in rats using a urine and serum metabolomics approach.* Sci Rep, 2017. **7**(1): p. 11433.
34. Li, Z., L.B. Agellon, and D.E. Vance, *Phosphatidylcholine homeostasis and liver failure.* J Biol Chem, 2005. **280**(45): p. 37798-802.
35. Kalhan, S.C., et al., *Plasma metabolomic profile in nonalcoholic fatty liver disease.* Metabolism, 2011. **60**(3): p. 404-13.
36. Stapelbroek, J.M., et al., *Liver disease associated with canalicular transport defects: current and future therapies.* J Hepatol, 2010. **52**(2): p. 258-71.
37. Roche, H.M., et al., *Isomer-dependent metabolic effects of conjugated linoleic acid: insights from molecular markers sterol regulatory element-binding protein-1c and LXRalpha.* Diabetes, 2002. **51**(7): p. 2037-44.
38. Erdinest, N., et al., *Anti-inflammatory effects of alpha linolenic acid on human corneal epithelial cells.* Invest Ophthalmol Vis Sci, 2012. **53**(8): p. 4396-406.
39. Degirolamo, C., et al., *Therapeutic potential of the endocrine fibroblast growth factors FGF19, FGF21 and FGF23.* Nat Rev Drug Discov, 2016. **15**(1): p. 51-69.
40. Zhao, Z.H., et al., *Ferulic acid is quickly absorbed from rat stomach as the free form and then conjugated mainly in liver.* Journal of Nutrition, 2004. **134**(11): p. 3083-3088.
41. Poquet, L., et al., *Transport and metabolism of ferulic acid through the colonic epithelium.* Drug Metabolism and Disposition, 2008. **36**(1): p. 190-197.
42. Lafay, S., et al., *Absorption and metabolism of caffeic acid and chlorogenic acid in the small intestine of rats.* Br J Nutr, 2006. **96**(1): p. 39-46.
43. Zhao, Z.H. and M.H. Moghadasian, *Chemistry, natural sources, dietary intake and pharmacokinetic properties of ferulic acid: A review.* Food Chemistry, 2008. **109**(4): p. 691-702.
44. Tapiero, H., et al., *Polyphenols: do they play a role in the prevention of human pathologies?* Biomedicine & Pharmacotherapy, 2002. **56**(4): p. 200-207.
45. Wiseman, H., et al., *Influence of 10 wk of soy consumption on plasma concentrations and excretion of isoflavonoids and on gut*

microflora metabolism in healthy adults. American Journal of Clinical Nutrition, 2004. **80**(3): p. 692-699.
46. Clavel, T., et al., *Phylogeny of human intestinal bacteria that activate the dietary lignan secoisolariciresinol diglucoside.* Fems Microbiology Ecology, 2006. **55**(3): p. 471-478.
47. Clavel, T., et al., *Intestinal bacterial communities that produce active estrogen-like compounds enterodiol and enterolactone in humans.* Appl Environ Microbiol, 2005. **71**(10): p. 6077-85.
48. Selma, M.V., et al., *Interaction between Phenolics and Gut Microbiota: Role in Human Health.* Journal of Agricultural and Food Chemistry, 2009. **57**(15): p. 6485-6501.
49. Olthof, M.R., et al., *Chlorogenic acid and caffeic acid are absorbed in humans.* J Nutr, 2001. **131**(1): p. 66-71.
50. Schmucker, D.L., *Age-related changes in liver structure and function: Implications for disease ?* Exp Gerontol, 2005. **40**(8-9): p. 650-9.
51. Le Couteur, D.G. and A.J. McLean, *The aging liver. Drug clearance and an oxygen diffusion barrier hypothesis.* Clin Pharmacokinet, 1998. **34**(5): p. 359-73.
52. Kim, I.H., et al., *Aging and liver disease.* Curr Opin Gastroenterol, 2015. **31**(3): p. 184-91.
53. Dong, S., et al., *Urinary metabolomics analysis identifies key biomarkers of different stages of nonalcoholic fatty liver disease.* World J Gastroenterol, 2017. **23**(15): p. 2771-2784.
54. Safaei, A., et al., *Metabolomic analysis of human cirrhosis, hepatocellular carcinoma, non-alcoholic fatty liver disease and non-alcoholic steatohepatitis diseases.* Gastroenterol Hepatol Bed Bench, 2016. **9**(3): p. 158-73.
55. Arteel, G.E., *Alcohol-induced oxidative stress in the liver: in vivo measurements.* Methods Mol Biol, 2008. **447**: p. 185-97.
56. Dodd, D., et al., *A gut bacterial pathway metabolizes aromatic amino acids into nine circulating metabolites.* Nature, 2017. **551**(7682): p. 648-652.
57. Kim, M.H., et al., *A Metagenomic Analysis Provides a Culture-Independent Pathogen Detection for Atopic Dermatitis.* Allergy Asthma Immunol Res, 2017. **9**(5): p. 453-461.
58. Yoo, J.Y., et al., *16S rRNA gene-based metagenomic analysis reveals differences in bacteria-derived extracellular vesicles in the urine of pregnant and non-pregnant women.* Exp Mol Med, 2016. **48**: p. e208.
59. Shen, Y., et al., *Outer membrane vesicles of a human commensal mediate immune regulation and disease protection.* Cell Host Microbe, 2012. **12**(4): p. 509-20.
60. Choi, Y., et al., *Gut microbe-derived extracellular vesicles induce insulin resistance, thereby impairing glucose metabolism in skeletal muscle.* Sci Rep, 2015. **5**: p. 15878.

61. Zhang, L.S. and S.S. Davies, *Microbial metabolism of dietary components to bioactive metabolites: opportunities for new therapeutic interventions.* Genome Med, 2016. **8**(1): p. 46.
62. Tang, M., et al., *Effect of Vitamin E With Therapeutic Iron Supplementation on Iron Repletion and Gut Microbiome in US Iron Deficient Infants and Toddlers.* J Pediatr Gastroenterol Nutr, 2016. **63**(3): p. 379-85.
63. Ruiz, L., et al., *Bile resistance mechanisms in Lactobacillus and Bifidobacterium.* Front Microbiol, 2013. **4**: p. 396.

국문 초록

서론: Ursodeoxycholic acid (UDCA)는 1 차 담즙산이 장내세균에 의해 생성되는 2차 담즙산이다. 본 약물은 원발성 담즙성 간경변 (Primary Biliary Cholangitis)의 치료제로는 미국 FDA (Food and Drug Administration)가 허가 승인한 유일한 약물이다. 원발성 담즙성 간경변의 근본적인 치료법은 간 이식으로 UDCA 투약을 통해 증가된 간 수치를 감소시킬 수 있으나, 이에 대한 정확한 기전은 밝혀지지 않았다. 본 연구에서는 건강한 성인 남성 및 노인, 간 기능 저하 환자에게 UDCA 투약을 통해 간 기능 보호 효과 및 보호 기전을 대사체 분석을 통해 확인하고자 하였다.

방법: 건강한 성인 남성 24 명과 노인 24 명, 간 기능 저하 환자 20 명이 본 연구에서 모집 되었다. 건강한 성인 남성 자원자에게 400, 800, 또는 1200 mg 의 UDCA 를, 노인 자원자에게는 400 또는 800 mg 의 UDCA 를 매일 1 회씩 2 주 투약하였다. 간 기능 저하 환자에게는 UDCA 800 mg 또는 비타민 E 800 IU 을 매일 1 회씩 8 주 투약하였다. 투약 전과 투약 종료시점에서 혈액과 소변을 수집하였고 내인성 대사체 분석을 위해 Liquid chromatography coupled with quadrupole time-of-flight mass spectrometry (LC-QTOFMS)와 gas chromatography coupled with time-of-flight mass spectrometry (GC-TOFMS)를 사용하였다. 15 개의 담즙산 정량을 위해서는 liquid chromatography tandem mass spectrometry 가 사용되었다.

결과: 건강한 자원자는 2 주간의 UDCA 투약을 통해 alanine transaminase (ALT), aspartate aminotransferase (AST) 그리고 혈청 간독성 마커중 하나인 miR-122 가 투약 전 대비 유의하게 감소함을 확인할 수 있었다. 소수성 담즙산 중 하나인 tauro-deoxycholoic acid 도 투약 후 감소하였다. LC- 그리고 GC-기반 비표적 대사체 분석에서는 아미노산, 플라보노이드 그리고 다양한 지방산에 속하는 대사체들이 투약 전 후 혈청과 소변에서 변화하였다. 노인 자원자에서는 UDCA 400 mg 을 투약한 군에서만 2 주 뒤 ALT 가 유의하게 감소하였으나 그 외의 간 기능 지표 및 대사체 프로파일링에서 유의한 변화는 없었다. 마지막으로 간 기능 저하 환자의 경우, 8 주간의 UDCA 투약 후 혈청 ALT, AST, gamma-glutamyl transferase 그리고 혈청 miR-122 가 감소하였고, 소수성 담즙산 deoxycholic acid 의 농도 또한 투약 전 대비 유의하게 감소하였다. 비표적 대사체 분석에서는 UDCA 투약을 통해 요독성을 띄는 내인성 대사체들이 감소, 항산화 효과가 있는 대사체들이 증가하였고 이러한 효과는 phenylalanine/tyrosine pathway 와 밀접한 관계가 있음을 확인하였다. 장내미생물 유래소포의 메타게놈 시퀀싱을 통해서 *Lactobacillus* 와 *Bifidobacterium* species 의 양이 UDCA 의 투약에 의해 유의한 감소를 보였다.

결론: 단기 UDCA 투약으로 간 기능 수치 개선 및 소수성 담즙산 감소효과를 확인 할 수 있었고, 이런 UDCA 의 간 기능 보호 기전은

장내미생물 및 대사물질 경로 조절을 통해 이루어 질 수 있음을 확인하였다.

* 본 내용의 일부는 *Scientific Reports* 학술지 (Da Jung Kim, et al. Sci. Rep. 8, 11874 (2018). DOI: 10.1038/s41598-018-30349-1)와 *Metabolomics* 학술지 (Da Jung Kim, et al. Metabolomics. (2019) 15:30. DOI: 10.1007/s11306-019-1494-5)에 출판된 내용임.

주요어 : 우루소데옥시콜린산, 비표적 대사체학, 표적 대사체학, 간 기능 이상, 간보호 기전

학 번 : 2015-31231